

1 **Model-based study of the role of rainfall and Land Use**
2 **Land Cover in the changes in Niger Red floods occurrence**
3 **and intensity in Niamey between 1953 and 2012.**

4
5 **C. Casse¹, M. Gosset¹, T. Vischel², G. Quantin², B. A. Tanimoun³**

6 [1]{Géoscience Environnement Toulouse (UMR 5563 CNRS, IRD, Université Toulouse III),
7 Observatoire Midi-Pyrénées, Toulouse, France}

8 [2]{Laboratoire des Transferts en Hydrologie et Environnement (UMR 5564, CNRS, IRD,
9 Université Grenoble I), France}

10 [3]{Autorité du Bassin du Niger (ABN), Niamey, Niger}

11 Correspondence to: C. Casse (claire.casse@get.obs-mip.fr) and M. Gosset
12 (marielle.gosset@ird.fr)

13

14 **Abstract**

15 Since 1950, the Niger River basin went through 3 main climatic periods: a wet period (1950-
16 1960), an extended drought (1970-1980) and since 1990 a partial recovery of the rainfall.
17 Hydrological changes co-occur with these rainfall fluctuations. In most of the basin the
18 rainfall deficit caused an enhanced discharge deficit, but in the Sahelian region the runoff
19 increased despite the rainfall deficit. Since 2000, the Sahelian part of the Niger has been hit
20 by an increase of flood hazards during the so-called Red flood period. In Niamey city, the
21 highest river levels and the longest flooded period ever recorded occurred in 2003, 2010, 2012
22 and 2013, with heavy casualties and property damage. The reasons for these changes, and the
23 relative role of climate versus Land Use Land Cover (LULC) changes are still debated and are
24 investigated in this paper. The evolution of the Niger Red flood in Niamey from 1950 to
25 2012 is analysed based on long-term records of rainfall (three data sets based on in situ and/or
26 satellite data) and discharge, and a hydrological model. The model is firstly run with present
27 LULC conditions in order to analyse solely the effect of rainfall variability. The impact of
28 LULC and drainage area modification is investigated in a second step. The simulations based
29 on the current surface conditions are able to reproduce the observed trend in Red flood

1 occurrence and intensity since the 1980s. This has been verified with three independent
2 rainfall data sets and implies that rainfall variability is the main driver for the Red flood
3 intensification observed over the last 30 years. The simulation results since 1953 reveals that
4 LULC and drainage area changes need to be invoked to explain the changes over a 60 year
5 period.

6

7 **1 Introduction**

8 The Sahel region has overcome drastic changes over the last 60 years. The long drought that
9 occurred in the 1970s and 1980s (Lamb 1982, Le Barbé and Lebel 1997, Nicholson et al.
10 2000, Camberlin et al. 2002, Le Barbé et al. 2002, L'Hôte et al. 2002, Dai et al. 2004, Lebel
11 and Ali 2009, Panthou et al. 2014) is considered as one of the strongest climatic signal of the
12 20th century (L'Hôte et al. 2002, Dai et al. 2004, Narisma et al. 2007). In addition to dramatic
13 consequences on the population, this drought induced long-term changes on the eco- and
14 hydrosystems. Since the 1990s the region has come back to wetter conditions even though the
15 annual rainfall is not back to the levels reached in the 1950s or 1960s. This recent partial
16 recovery is heterogenic over the Sahel, with dry conditions persisting in the western part
17 (Nicholson et al. 2000, L'Hôte et al. 2002, Dia et al. 2004, Lebel and Ali 2009, Panthou et al.
18 2014). In the Central-East Sahel the rainfall deficit is dropping over the last decade,
19 interannual variability is strong (Dai et al. 2004) and rainfall appears more intense (more
20 extreme events) than in the 1950s and 1960s (Panthou et al. 2014).

21 Concurrent with these climatic variations West Africa has experienced major hydrological
22 changes. The Niger (Fig. 1) is the largest river of West Africa and goes through a strong
23 climatic gradient from the humid Guinean region to the sub-desertic Sahara and through the
24 semi-arid Sahel. The hydrological response to the extended drought of the 1970s-1980s has
25 been different in the various sub-regions of the Niger basin. In the Guinean region the
26 discharge deficit was twice as important as the rainfall deficit (Briquet et al. 1996, Mahé et al.
27 2000, Mahé 2009, Paturel et al. 2010). After the 1970s-1980s the discharge deficit of the Bani
28 (the main tributary of upper Niger River) compared to the 1950s reached 80% (Mahé et al.
29 2000). During the same dry years the phenomenon known as "Sahelian paradox" (Descroix et
30 al. 2009) was observed in many part of the Sahel: an increase in runoff despite the deficit in
31 rainfall (Albergel 1987, Amani and Nguetora 2002, Mahé et al. 2003, 2005, 2009). This

1 phenomenon resulted in a discharge increase in exoreic¹ basins (Amani and Nguetora 2002,
2 Mahé et al. 2003, 2005, 2009, Descroix et al. 2009, Amogu et al. 2010) and in larger pond
3 surfaces, infiltration and water table levels in the endorheic² areas (Desconnet et al. 1997,
4 Leduc et al. 2001, Favreau et al. 2009, Gardelle et al. 2010).

5 The discharge of the Niger River in Niamey (Fig. 1), the capital city of Niger, is impacted by
6 the hydrological behaviour of both the upper Niger basin and of the Sahelian tributaries. The
7 rainfall in the upper Niger triggers the “*Guinean flood*”, which propagates slowly and occurs
8 in Niamey after the rainy season (around January) (Millot 1913, Pardé 1933, Descroix et al.
9 2012, Sighomnou et al. 2013). The rainfall drained by the Sahelian tributaries in the vicinity
10 of Niamey, superimposes on the Niger River flows and triggers the “*Red flood*”; “red” refers
11 to the colour of the water loaded in iron oxide sediment during this period (Millot 1913, Pardé
12 1933, Descroix et al. 2012, Sighomnou et al. 2013). Before the rainfall deficit of the 1970s-
13 1980s the hydrograph in Niamey was single peaked; the *Red flood* was low and almost
14 merged with the *Guinean flood*. Gradually after the 1970s-1980s, the runoff increased in the
15 Sahelian tributaries and enhanced their contribution to the *Red flood*. Consequently the
16 hydrograph in Niamey evolved from a “one peak” to a “two peaks” shape (Amani and
17 Nguetora 2002, Mahé et al. 2003, Amogu et al. 2010, Sighomnou et al. 2013). Descroix et al.
18 (2012) poetically described this phenomenon as “the dromedary became a camel”. The
19 increasing intensity of the *Red flood* in the last decade has enhanced the inundation risk,
20 causing dramatic human and material losses. In 2003, 2010, 2012 and 2013 water levels and
21 duration of the inundation were the highest ever recorded since the beginning of observations
22 in 1920 (Sighomnou et al. 2013).

23 The reasons for this dramatic increase in the flood risk in Niamey are still debated by the
24 scientific community. Previous studies, based on observations only, have shown the
25 correlation between the drastic changes in the surface and vegetation conditions in Sahelian
26 sub-basins and the changes in their hydrological behaviour, like an increase in runoff. These
27 processes have been proposed as an explanation for the observed changes in Niamey
28 hydrograph's. In Sahel, runoff is mainly controlled by surface conditions (Collinet et
29 Valentin, 1979, Albergel et al. 1987, Cazenave et Valentin, 1992), which have been changing

¹ where the hydrographic network does connect to a river and or to the ocean

² where the hydrographic network does not connect to a river

under climatic (Hiernaux and Le Houérou 2006, Leblanc et al. 2008) and anthropic pressure - wood harvesting (Peltier et al. 1995, Leblanc et al. 2008) or crop extension (Valentin et al. 2004). Several authors (Amani and Nguetora 2002, Mahé et al. 2003, Leblanc et al. 2008, Amogu et al. 2010, Descroix et al. 2009, 2012, 2013) have highlighted that hydrological changes in Niamey hydrograph could be triggered by the **Land Use and Land Cover (LULC) changes** (and the resulting runoff increase) that have occurred since the 1970s in the three main tributaries of the Niger responsible of the Red flood in Niamey (the Gorouol, Dargol and Sirba rivers). Recently small scale **changes in the hydrographical network** in the vicinity of Niamey have been put forward as a possible driver for *Red flood* increase (Amogu et al. 2010, Descroix et al. 2012, Mamadou et al. 2015). In some parts of the Niger left bank, which used not to contribute to the river (endoreism), heavy runoff has increased the network connection (Leblanc et al. 2008, Amogu et al. 2010) and opened new water channels to the main river. The role of a **changing rainfall regime** in the flood risk increase is also an open question (Nka et al. 2015). Recent studies suggest that rainfall has intensified in the Central Sahel (Panthou et al, 2014). In a region where the runoff is very dependent on high rainfall intensities (Vischel and Lebel 2007, Casse et al. 2015) a strong hydrological response to rainfall extremes is expected. The present paper does not intend to provide new evidence about these changes but rather to investigate their impact on the hydrological regime. The interactions and co-occurrence of the LULC, water pathway and rainfall changes over the past decades, makes it difficult to attribute the flood risk increase on the basis of observations alone. Unlike the intricate reality, models allow testing the influences of each process or variable independently. Many authors used hydrological modelling (based on different scale, basin, data set and model) to infer the role of climate and LULC on hydrological changes in West Africa since 1950 (1950-1998: Seguis et al. 2004, 1951-2000: D'Orgeval and Polcher 2008, 1950-2009: Aich et al. 2015). The conclusions differ among these studies: D'Orgeval and Polcher (2008) found that LULC was less important than rainfall changes, in contrast to Seguis et al. (2004), while Aich et al. (2015) concluded on the role of both LULC and climate. Casse and Gosset (2015) presented a preliminary work between 1983 and 2012, and showed that rainfall variability alone could explain the observed changes in the Niger river hydrograph in Niamey over the last 30 years. Only Aich et al. (2015) and Casse and Gosset (2015) focused on the Sahelian Tributaries of the Niger and the Niamey station. Both studies based their conclusion on one rainfall dataset, Aich et al. (2015) using a re-analysis product and Casse and Gosset (2015) a satellite rainfall product (PERSIANN-CDR).

1 Following the preliminary work of Casse and Gosset (2105), this paper aims to better
2 understand the role of the tree main identified environmental changes that could drive the
3 hydrological evolution of the Niamey *Red flood* from 1950 to 2012. This study is based on
4 long-term records of rainfall and discharge, and a hydrological model. It investigates the
5 sensitivity of the hydrological response to rainfall variability, LULC and drainage area
6 changes. The model is first run with present LULC and drainage area conditions in order to
7 analyse solely the effect of rainfall variability. The impact of LULC and drainage area
8 modification is investigated in a second step. The numerical experiment is first carried out
9 over the 1983-2012 period, where 3 different rainfall products are available, to verify that
10 conclusions on the role of rainfall changes are robust and independent of the data set. The
11 changes since 1950 are then analysed using the only data set available for the extended period
12 (based on rain gauges). The originality of this paper compared to previous studies lies in: (i)
13 the time period that includes the 2010 and 2012 record *Red floods*, (ii) the various rainfall
14 products used, (iii) the study of the basin area changes, (iv) and the decadal approach to
15 analyse the long-term changes.

16 Section 2 describes the study area, the data and the hydrological model set up. Section 3
17 presents the observed changes in rainfall and discharge over 1950-2012. Section 4 analyses
18 the hydrological model outputs, compares the simulated and observed changes over the six
19 decades, and discusses the sensitivity to LULC and drainage area changes. Section 5 gives the
20 conclusions about the role of rainfall variability and other drivers of change in the increase of
21 the *Red flood* events since the 1950s.

22

23 **2 Data and method**

24 **2.1 Study area and hydrological context**

25 This study focuses on the area where the runoff responsible for the Red flood is produced.
26 This area is situated in the middle Niger basin, in the Sahelian belt, between Ansongo
27 (15°40'N, 0°30'E, Mali) and Niamey (13°31'N, 2°6'E, Niger) as contoured in red in Fig.1
28 (top left panel). The right bank of the Ansongo-Niamey reach collects 3 main tributaries (Fig.
29 1 bottom lef pannel): the Gorouol (in Alcongui), the Dargol (in Kakassi) and the Sirba (in
30 Garbey). These are the first tributaries of the Niger river since the inner delta. The Gorouol,
31 Dargol and Sirba are ephemeral rivers, named koris, which flow only during the rainfall

1 season. The left bank of the Niger in the study zone is mainly endorheic. The hydrographical
2 network is organised in connected ponds and the runoff does not contribute much to the Niger
3 river. Amogu et al. (2010) and Mamadou et al. (2015) have reported however that in parts of
4 the left bank the hydrographical network is changing and water channels are created down to
5 the main river bed; the phenomenon is known as “endorheic rupture” and increases the runoff
6 contribution from the left bank to the Niger main stream.

7 Figure 2 displays the discharge recorded at Ansongo and Niamey gauging stations in 2012
8 and 1955. 2012 is a good illustration of a strong *Red flood* event in Niamey. As discussed in
9 the introduction and visible in Fig. 2b, the discharge in Niamey is the superposition of the
10 Guinean flood, arriving from the upper Niger basin (as seen at Ansongo, Fig. 2a) and of the
11 additional runoff generated in the Gorouol, Dargol and Sirba basin between July and October.

12 **2.2 Discharge data**

13 Five discharge gauging stations within the studied zone are used to analyse the observed
14 changes and also as input or validation for the model simulations. Ansongo (Mali) at the head
15 of the study zone is needed to analyse the *Guinean flood* before any influence of the Red
16 flood on the discharge. Ansongo data is also needed as input to the hydrological model (see
17 below). The discharge in Niamey is the main focus of this work, and is the best quality data
18 record of all five stations. It is also the only station used to validate the model output. The
19 discharge at the 3 right bank tributaries outlets (Alcongui, Kakassi and Garbey) is used to
20 quantify the locally generated runoff and its variability over the years. All discharge data is
21 provided by the Niger Basin Authority (ABN) data base. The data set covers 60 years from
22 1953 to 2012 for Ansongo and Niamey (with a significant number of missing data during low
23 flows water in Ansongo during 1960s and 1990s), and 1957-2012 period for Alcongi, Kakassi
24 and Garbey stations with 28 complete common years (1957, 1963 to 1975, 1977, 1979, 1980,
25 1982 to 1987, 2006 to 2008 and 2012).

26 **2.3 Quantifying the *Red flood* contribution to Niamey's discharge**

27 As the study focuses on the *Red flood* in Niamey, a first challenge is to isolate this flood from
28 the *Guinean flood* in the Niamey discharge, based on available observations. For recent years,
29 where the two floods are clearly independent (Fig. 2b), an automatic algorithm based on
30 maxima detection can be implemented. For distant years where the two floods were almost

1 merged (Fig. 2d) the task is difficult. A two-step method suitable for both merged and non-
2 merged flood hydrographs is implemented. First, the period where the runoff leading to *Red*
3 *flood* occurs is delimited. Second, the *Red flood* contribution is quantified based on
4 comparing Niamey's and Ansongo's discharge.

5 For each year the *Red flood* period is delimited based on the observed rainy season, as
6 illustrated with the vertical lines in Fig. 2 (b an d). The longest rainfall record, available for
7 the whole 1953-2012 period is used (see Sec. 2.4 below). The starting date of the *Red flood*
8 period is set as the day when 10% of the annual rainfall amount is reached. The end date is set
9 to the day when 98% of the annual rainfall is reached plus a 10 day margin. The margin
10 accounts for the time needed for runoff over the entire drainage area to reach Niamey.

11 Once the *Red flood* period is delimited, the next step is to quantify the proportion of Niamey's
12 discharge attributable to runoff in the Ansongo-Niamey sub-basin, from what is propagating
13 from the upper basin. Two methods have been used. The first method assumes that the main
14 runoff contribution between Ansongo and Niamey comes from the 3 right bank tributaries.
15 With this assumption the sum of the 3 discharges can be used as a proxy. This method
16 however occults the contribution of direct rainfall over the river bed or runoff from the left
17 bank. Also the station records are not available on the entire studied period. The second
18 method is based on subtracting the Ansongo's discharge to the Niamey's discharge. Note that
19 during the *Guinean flood* (Fig. 2 a and c) the discharge in Ansongo is higher than in Niamey
20 (Fig. 2 b and d). The source of this loss is not yet understood; according to ABN experts it
21 may come both from evaporation and water loss through bedrock fractures or flush back from
22 Niger main stream into dry koris after the rainy season. This loss must be accounted for,
23 before subtracting Ansongo's to Niamey's discharge. To do so, Ansongo's discharge is
24 morphed to fit the shape of the *Guinean flood* as observed in Niamey. This is illustrated by
25 the difference between the dash line in Fig 2b (resp. 2d) and the plain line in Fig 2a (resp. 2c).
26 Then, the local *Red flood* contribution is estimated as the area between Niamey's discharge
27 (black line in Fig 2b) and Ansongo's morphed discharge (dash line), between the beginning
28 and end of the *Red flood* period (vertical blue lines in Fig 2b).

29 Whatever the method used, the estimation of local runoff production is prone to uncertainty.
30 In method one (sum of 3 tributaries discharge) the errors may come from the quality of the
31 data record and ignoring rainfall over the river bed and the left bank. In method two, most of
32 the error comes from the quality of the data record in Ansongo and also from the difficulty to

1 quantify the losses in the discharge between Ansongo and Niamey. In any case, the objective
2 here is not an accurate quantification of the runoff every year but rather the analysis of the
3 main trends and relative changes over 60 years.

4 **2.4 Rainfall data record**

5 Rainfall data is used in Sec. 3 to analyse the observed changes in the climatic and
6 hydrological signals. It is also needed as forcing for the hydrological model.

7 Rainfall over the Niger basin is associated with the West African Monsoon and falls mainly
8 between June and October. In the studied area, like in overall Sahel, 90% of rainfall comes
9 from propagating Meso-scale Convective Systems (MCS) (Laurent et al. 1998, Mathon et al.
10 2002, Lebel et al. 2003). Although MCS patterns vary, they often organize in a curved
11 convective line followed by a stratiform region (Houze 1993). The resulting rain fields are
12 characterized by strong space-time variability, with intense rain rates when the convective
13 front is passing through (typically during less than an hour in a given point at ground)
14 followed by a few hours of less intense rainfall in the stratiform part. Reproducing this highly
15 spatially and temporally variable patterns is a challenge for the different rainfall products.
16 This is an important point when forcing models because the hydrological response depends
17 not only on the accumulations but also on the distribution of rainfall in time, space, and
18 intensity classes (Gosset et al. 2013, Casse et al. 2015). Three rainfall data records have been
19 used in this work (Table 1). All three are spatialized rainfall products, provided on a regular
20 grid and well suited for forcing a distributed hydrological model. Two of the products are
21 based on rain gauge information and one on satellite information. The three products are
22 described below. The appendix A compares the three products and confronts them with a
23 reference, both in terms of rainfall amount and distribution (in time, space and intensity).

24 **2.4.1 “KRIG”: a research product based on a rich set of operational gauges**
25 **(available since 1950)**

26 This regional product provided by the Laboratoire des Transfert en Hydrologie et
27 Environnement (LTHE), hereafter named KRIG product, is a gauge based rainfall estimate.
28 This product is based on a data base first built by Le Barbé et al. (2002) and updated by
29 Panthou et al. (2014). KRIG product is based on rain gauge records from different institutes:
30 the Centre Inter-Etats d’Etudes Hydraulique (CIEH), the AGRometeorology, Hydrology,

1 METerology centre (AGRYMET) and the National Weather services from several African
2 countries (DMN in French). The available network density is variable during the period and
3 inside the basin. Over the studied area and after quality control, the available number of
4 stations ranges from 60 to 15 gauges between 1950 and 2012, and since 2006 the network is
5 sparser, with less than 30 gauges (Fig. 3). As in Vischel et al. 2011, the kriging technique is
6 used to interpolate the daily gauge information and provide a regularly gridded product with a
7 $0.5^{\circ} \times 0.5^{\circ}$ resolution. We checked the impact of the variation of the number of gauges over the
8 domain on the inter-annual trends in rainfall (presented in Sec. 3). We found (not shown) that
9 the main trend is not modified when using a network of only 10 gauges (those available for
10 the whole series).

11 2.4.2 “CPC”: an operational gauge product (available since 1979)

12 The National Oceanic and Atmospheric Administration (NOAA) Climate Prediction Centre
13 (CPC) provides the CPC Unified Gauge-Based Analysis of Global Daily Precipitation, here
14 after named CPC, and available on http://ftp.cpc.ncep.noaa.gov/precip/CPC_UNI_PRCP/GAUGE_GLB/ (both data and documentation). This daily- 0.5° product,
15 available from 1979 to present, is based on the Gandin (1965) optimal interpolation which
16 according to Chen et al. (2008) provides a robust global precipitation estimate in different
17 condition of climate, season and network density. On the contiguous United States a
18 correlation of 0.5 was found between the referenced network (30km station-to-station
19 distance) and a synthetic sparse network which mimics tropical Africa situation (400km
20 station-to-station distance) (Chen et al. 2008). On the Ansongo-Niamey reach basin, the
21 annual mean number of gauges has been increasing over the period and ranges from 1.5
22 (1980) to 6.2 (2010) (Fig. 3). This density is very low compared to the density provided by
23 the KRIG product above. Casse et al. (2015) however showed that a hydrological model
24 forced with CPC gave satisfactory results over the area for the 2000-2013 period, where the
25 annual mean number of gauges is around 5.2 (± 0.66).
26

27 2.4.3 “PERSIANN-CDR”: a satellite based product (available since 1983)

28 Based on the PERSIANN algorithm (Sorooshian et al. 2000) a new Climate Data Record
29 called PERSIANN-CDR (Ashouri et al. 2015) with a daily- 0.25° resolution is currently
30 available from 1983 to present (www.ncdc.noaa.gov/cdr/operationalcdrs.html). PERSIANN-
31 CDR is based on high temporal resolution infrared information from geostationary satellite

1 (GridSat-B1, from the International Satellite Cloud Climatological Project, ISCCP) and it is
2 bias corrected with the Global Precipitation Climatology Project (GPCP) monthly rainfall
3 estimates (Ashouri et al. 2015).

4 **2.5 Hydrological model and set up**

5 The hydrological simulation is based on the ISBA-TRIP model, already used in Casse et al.
6 (2015) and Casse and Gosset (2015) to study the Ansongo-Niamey reach of the Niger basin.
7 Casse et al. (2015) tested the model over the 2000-2013 period with a variety of rainfall
8 products. They showed that ISBA-TRIP was able to reproduce the frequency of *Red floods* in
9 the recent period. Casse and Gosset (2015) used the same model and the rainfall product
10 PERSIANN-CDR to study the 1983-2012 period, also with satisfactory results.

11 **2.5.1 The ISBA-TRIP coupled model**

12 Within the SURFEX modelling platform (developed by Météo France and standing for
13 SURFace Externalisée in French; www.cnrm.meteo.fr/surfex/, Masson et al. 2013), a Land
14 Surface Model (LSM) is coupled to a routing model.

15 The LSM, called ISBA (Interaction between Soil Biosphere and Atmosphere) computes the
16 water (and energy) balance based on the soil/vegetation properties of each grid cell and the
17 atmospheric forcing provided at each time step. Several options are available within ISBA to
18 produce runoff; here the production is based on a parameterization of sub-grid hydrology.
19 This allows to take into account the high spatial variability of rainfall and runoff processes
20 within a 0.5° cell (Decharme and Douville, 2005, 2007).

21 ISBA output feeds the routing model called TRIP (Total Runoff Integrating Pathway) which
22 turns surface runoff, ground water and floodplain water contributions into discharge for each
23 grid cell, and then propagates the surface flows through the river network. TRIP reservoirs
24 implemented in the version 6 of SURFEX (used in this study) are: the river, the ground water,
25 the flood plain, and the aquifer. Within these reservoirs, evaporation and infiltration occurs
26 only in flood plains. Distributed parameters (based on physical equation or on fixed values)
27 control the river hydrology: length, slope, width, depth, Manning coefficients of river and
28 flood plain, partitioning coefficient between groundwater and aquifer, return time of
29 groundwater and aquifer to the river.

1 For more precision on the ISBA-TRIP model physics please refer to Noilhan and Planton
2 (1989, first developers), Boone et al. (1999, for the soil layers physics), Decharme et Douville
3 (2005 and 2007, for the subgrid hydrology), Decharme et al (2006, for vegetation impact on
4 infiltration) or Pedinotti et al. (2012, for the implementation on the Niger basin).

5 The model is implemented on the Ansongo-Niamey reach basin (Fig. 4) with a grid resolution
6 of $0.5^{\circ} \times 0.5^{\circ}$ and a 3h time step for the atmospheric forcing. This configuration is described in
7 details in Casse et al. 2015 and Casse and Gosset 2015. The value of the daily discharge at the
8 head of the reach (Ansongo pixel) is needed as input. The observed discharge data at the
9 Ansongo station provided by the ABN is used for this purpose.

10 2.5.2 Atmospheric forcing

11 ISBA needs a classical atmospheric forcing (precipitation, temperature, pressure, humidity,
12 radiance and wind) to compute the water balance for each grid cell. Here the atmospheric
13 forcing, except for rainfall, is provided as a climatological mean value for each day. The daily
14 mean value was computed from the 2003-2012 period based on the WATCH Forcing Data
15 methodology applied to ERA-Interim data (WFDEI, Weedon et al., 2011, Weedon et al.
16 2014), reanalysed by Météo France (B. Decharme personal communication, 2013). Sensitivity
17 tests (not shown) have been run to verify the sensitivity of the model output to this
18 atmospheric forcing. The tests showed that using a climatological mean does not impact the
19 simulated discharge and does not change the characteristic of the simulated Red flood.

20 The rain forcing is provided by the three rainfall data sets described in 2.4, PERSIANN-CDR,
21 CPC and KRIG. Their native resolution (daily and 0.5° or 0.25° , Table1) differ from the
22 resolution of model forcing input (3h- 0.5°). Daily rainfall are thus disaggregated at a 3 hour
23 time step following a very simple process. Observation over the studied region, based on
24 dense gauges network (<http://www.amma-catch.org/>) and meteorological radar
25 (<http://meghatropiques.ipsl.polytechnique.fr/the-ouagadougou-super-site.html>), shows that
26 daily rainfall is concentrated in a few hours. This observation is in accordance with previous
27 studies on MCS dynamic (Eldridge 1957, Rowell et Milford 1993). For the model forcing the
28 daily rainfall accumulation is condensed in one 3h time step (between 16 and 19pm), as in
29 Casse and Gosset (2015). The 0.25° resolution product (PERSIANN-CDR) is spatially
30 aggregated by spatial mean.

1 Since the model is not calibrated for each product, the differences between the 3 simulations
2 are due to differences between the rain products (Appendix 1). Using 3 independent rainfall
3 dataset will consolidate the conclusions concerning the role of rainfall changes on hydrology.

4 **2.5.3 Vegetation map**

5 ISBA computes energy and water balance, based on empirical equation and vegetation and
6 soil properties. In the reference simulation the vegetation map (vegetation type and fraction,
7 Fig. 4a) is based on the Ecoclimap data (Masson et al. 2003, which cover the 2002-2006
8 period) and the soil texture (sand, silt proportion) is based on FAO data. These data sets are
9 considered as representative of the current situation in the area. The bare sol proportion on the
10 basin ranges from 20 to 100% and follows the rainfall latitudinal gradient with less vegetation
11 in the north than in the south. Within ISBA, the vegetation cover of the Ansongo-Niamey
12 reach basin is composed mainly of Sahelian savannah and bush Sahelian savannah, which
13 present low coverage (LAI < 2 and at least 20% of bare soil). Contrary to landscape
14 description found in the literature (Amogu et al. 2010, Descroix et al. 2012), Ecoclimap data
15 does not consider any croplands in the study area. However sensitivity studies (not shown)
16 have highlighted that the model is sensitive to the vegetation cover fraction (LAI and
17 proportion of bare soil) rather than to the vegetation type (crop vs no crop). Thus LULC
18 changes impact on hydrology is explored by changing the vegetation cover fraction.

19 The simulations over the whole 1953-2012 period are first run with the current soil/vegetation
20 characteristics (Fig 4a), with the objective to analyse only the impact of rainfall regime
21 changes. In a second step the vegetation cover fraction is changed to be more representative
22 of the beginning of the period, with less area covered by bare soil and more wood (Fig 4b).

23

24 **3 Observed rainfall and hydrological changes since 1950s**

25 This section summarizes the hydrological and climatic changes observed over the study area
26 since the 1950s. The analysis is based on the inter-annual series of the normalized rainfall
27 index and similar indexe computed for the discharge. The normalized rainfall index, for a
28 series of N annual rainfall accumulation values R_i (here N=60) is defined each year i by:

29
$$I_i = \frac{R_i - \bar{R}}{\sigma_R} \quad (1)$$

1 where \bar{R} and σ_R are the mean and the standard deviation of the R_i series. The rainfall index is
2 based on the KRIG rainfall estimates (the only product available over the entire period).

3 The variability of the discharge in Niamey is analysed in the light of the variability of its two
4 components: (i) the Guinean flow arriving through Ansongo and (ii) the runoff generated over
5 the Ansongo-Niamey sub-basin. These indexes have been computed from the following *Red*
6 *flood discharge time series*:

- 7 • the annual mean discharge in Ansongo (in m^3s^{-1}),
- 8 • the annual mean discharge in Niamey (in m^3s^{-1}),
- 9 • the annual mean differential discharge, computed as the difference between the
10 Niamey and the morphed Ansongo discharges,
- 11 • the annual mean of the sum of the discharges from the 3 tributaries (Dargol, Sirba and
12 Gorouol).

13 As discussed in Sec. 2.3 the two last variables are proxies to the local runoff contribution to
14 Niger discharge.

15 Figure 5 illustrates the rainfall and hydrological changes in the Ansongo-Niamey reach basin
16 through 6 decades, from 1953 to 2012.

17 Figure 5a shows that the 1950s and 1960s are the wettest decades of the studied period (all
18 years present a positive rainfall index), followed by two decades with rainfall deficit in the
19 1970s and 1980s (starting in 1968). Since the 1990s the rainfall index presents strong
20 interannual variability; it is higher than in the dry period but still below the wettest decades.
21 These results, derived for the Ansongo-Niamey reach basin with the KRIG rainfall data set,
22 are consistent with the 3 main climatic periods the Sahelian region has undergone since 1950
23 (Lamb 1982, Le Barbé et Lebel 1997, Nicholson et al. 2000, Camberlin et al. 2002, Le Barbé
24 et al. 2002, L'Hôte et al. 2002, Dai et al. 2004, Lebel et Ali 2009, Panthou et al. 2014). Both
25 wet and dry decades were observed and the heterogenous rainfall recovery highlighted by
26 several authors (Nicholson et al. 2000, L'Hôte et al. 2002, Dia et al. 2004, Lebel and Ali
27 2009, Panthou et al. 2014) is confirmed over the studied area.

28 Figure 5b, c and d illustrate the inter-annual variability of respectively, the mean discharge in
29 Niamey during the *Red flood* period (Fig. 5d), and its two contributors: the Guinean flow as
30 recorded in Ansongo (Fig. 5b) and the local runoff (Fig. 5c). In Fig. 5c the two proxies used

1 to quantify local runoff contribution to the discharge (Sec. 2.3) are displayed. The grey shade
2 is for the index computed from the differential discharge between Ansongo and Niamey, the
3 yellow colour is for the index based on the sums of the tributaries. The gaps in the latter series
4 are due to missing data.

5 As expected, the trends in the Ansongo discharge variability are consistent with what is
6 known of rainfall variability in West Africa and Sahel over the last 60 years: the wet decades
7 of the 1950s and 1960s are associated with the highest discharge index, the long period with
8 negative index during the 1970s and 1980s highlights the decrease in discharge during the
9 drought in the upper Niger basin. From the 1990s the discharge index have increased again
10 but are still lower than in the 1950s-1960s wet conditions and shows an enhanced inter-annual
11 variability.

12 In contrast with the relatively similar trends displayed by rainfall (Fig. 5a) and the Ansongo
13 discharge (Fig. 5b) the index for the local runoff contribution (Fig. 5c) shows a very different
14 evolution over the 6 decades. The salient feature is an increase over the period with mostly
15 negative values until the mid 1980s and increasing positive values afterwards. Given the
16 many sources of uncertainty in deriving the two proxies (Sec. 2.3) the agreement is quite
17 remarkable and shows that the observed trend is robust. Both proxies agree that wet decades
18 present smaller index than drier ones; indicating that runoff in the Ansongo-Niamey basin
19 tends to increase over the entire studied period, with a sharp increase since the 1990s. This
20 result reflects the paradoxical behaviour of Sahelian basins described by several authors
21 (Albergel 1987, Amani and Nguetora 2002, Mahé et al. 2003, 2005, Mahé et Paturel 2009,
22 Descroix et al. 2009, 2012, Sighomnou et al. 2013). Previous studies have attributed the
23 changes in runoff coefficient to the effect of LULC changes (Seguis et al. 2004, Leblanc et al.
24 2008, Descroix et al. 2009, 2012). The reason for the sharp increase in runoff since the 1990s
25 and the possible role of rainfall intensification is debated in the community. Analysis at the
26 yearly scale, as presented above does not allow to conclude. The model based simulations in
27 the next section shine some light on these questions.

28 As expected, Niamey *Red flood* (Fig. 5d) changes over 1953-2012 reflect the influence of the
29 flow coming from the upper basin (Fig. 5b) and local contributions (Fig. 5c). In the 1950s and
30 1960s when the upper flow is high but local runoff is small, the mean discharge index is
31 average, with a succession of positive and negative years. During the 1970s and 1980s
32 drought it reaches the lowest values. In the recent period when the index for the upper basin

1 flow is average but local runoff is increasing sharply, the *Red flood* levels increase drastically
2 and reach their highest values.

3

4 **4 Model based analysis, sensitivity tests and attribution of the changes**

5 This section presents the modelling results and their ability to reproduce the hydrological
6 changes discussed in the previous section. First for the entire simulated period (1953-2012)
7 the soil/vegetation parameters and drainage area are held constant and are in agreement with
8 the present conditions (Fig. 4a). The only source of variability is the discharge in Ansongo and
9 the rainfall forcing. If this simulation is able to reproduce the hydrological observed changes,
10 then rainfall variability can be considered as the main driver for the hydrological changes. If
11 not, other possible drivers such as LULC and drainage area should be explored. The results
12 are first presented for 1983-2012 when 3 different rainfall forcing are available. The
13 simulations since 1953, which KRIG rainfall only, are then presented.

14 **4.1 1983-2012 period**

15 **4.1.1 Mean decadal hydrograph**

16 The mean decadal hydrograph is a good synthetic indicator of the salient changes in the
17 hydrological regime between the decades. The observed and simulated decadal hydrograph
18 for the last 3 decades (1983-1992, 1993-2002 and 2003-2012) are presented in Fig. 6.
19 According to Fig. 6a the observed discharge has globally increased through the 3 decades,
20 both in term of flood length and intensity. The increase in the *Guinean flood* (November to
21 May) is consistent with the increase in the Ansongo discharge already discussed (Fig. 5b).
22 The progressive apparition of the *Red flood*, clearly separating from the *Guinean flood* in the
23 last decade (2003-2012) is visible in Fig. 6a. The decadal mean of the total water volume
24 during the *Red flood* (integration of Niamey discharge during the *Red flood*), raised from 5.1
25 to 8.9 km³ during the 3 observed decades (Table 2). The enhancement of the Red flood due to
26 the combined effect of an increase in the upper basin flow (Fig. 5b) and local runoff (Fig. 5c)
27 is visible on the decadal hydrographs.

28 The simulated decadal mean hydrographs, based on the 3 rainfall forcing – KRIG, CPC and
29 PERSIANN-CDR – are able to reproduce the main features of the observed changes: the *Red*
30 *flood* increase and the progressive bi-modal shape reinforcement (Fig. 6b, c, d and Table 2).

1 Results show also discrepancies among the 3 simulations: KRIG rainfall leads to a smoother
2 simulated *Red flood* than CPC and PERSIANN-CDR which tend to overestimate the observed
3 discharge. As developed in Appendix A, the 3 rainfall data sets estimate well the annual
4 rainfall amount but distribute it differently in time, space and intensity. As already highlighted
5 in Casse et al. (2015), this difference in rainfall distribution impacts the hydrological
6 response.

7 During the *Guinean flood*, all simulations overestimate the discharge. This systematic
8 overestimation is mainly due to the observed deficit between Ansongo and Niamey (Sec. 2.2),
9 which is not simulated by the current modelling.

10 4.1.2 Quantile-quantile analysis

11 The frequency distribution of the daily discharge during the *Red flood*, for each decade are
12 analysed. The simulated and observed distributions are compared in two ways: (i) first the
13 observations and simulations are compared decade by decade (Fig. 7), in order to verify the
14 ability of the model to reproduce realistic distributions of the daily discharge; (ii) then the
15 relative changes in the distributions, between decades, are analysed both for observations
16 (Fig. 8a) and for simulations (Fig. 8b, c and d).

17 The distribution comparison between simulated and observed daily *Red flood* discharge (Fig.
18 7) for the 3 decades, highlights that the simulations tend to overestimate the observed
19 discharge. This is true for CPC and PERSIANN-CDR for the whole distribution, and for
20 KRIG for low and medium values. This is confirmed in Table 2 with the values of the mean
21 decadal volume of the *Red flood*. The observed deficit between Ansongo and Niamey, which
22 is not simulated, may explain these overestimations. The differences among the 3 simulations
23 are due to differences in rainfall distribution among the 3 rain products (Appendix A). The
24 KRIG based simulation tends to underestimate the highest discharge values. This is due to the
25 tendency of this product to smooth rainfall fields in time (high number of rainy days with low
26 intensities). The CPC based simulation overestimates steadily the discharge because this
27 products provides high intensity and the rainfall fields are concentrated in time and space.
28 PERSIANN-CDR's behaviour lies between these two products.

29 Despite the overall positive bias, the simulations reproduce the observed relative changes
30 between the driest (1983-1992) and the most recent decade (2003-2012) (Fig. 8): an overall
31 increase of the discharge. For the 1993-2002 decade, simulations are too close to the 2003-

1 2012 distribution while in the observations the 1993-2012 distribution is closer to the driest
2 decade 1983-1993. Ansongo input discharge quality is lower during the 1990s which may
3 lead to more uncertainties in the 1993-2002 simulations.

4 These results show that with constant LULC and drainage area conditions, the simulations are
5 able to reproduce the main trends of the hydrological regime changes between 1983 and 2012:
6 the discharge increase and the *Red flood* reinforcement are well simulated. Interannual rainfall
7 variability can thus be considered as the main driver for the hydrological changes during
8 1983-2012 period, as already found in Casse and Gosset (2015). Here, the use of 3 different
9 rainfall products, based on different data sets, with different characteristics over the domain
10 (Appendix A), reinforce the results.

11 **4.2 1953-2012 period**

12 Over the 1953-2012 period, the observed mean decadal hydrograph (Fig. 9a) varies according
13 to the 3 climatic periods observed in Fig. 5a: (i) the highest discharge and longest high water
14 level season are observed during the wettest decades (1953-1962 and 1963-1972), (ii)
15 discharge decreases during the first dry decade (1973-1982) and reaches its lower level during
16 the driest decade (1983-1992), (iii) before rising up over the two last decades (1993-2002 and
17 2003-2012), but without reaching the 1950s-1960s levels. From 1953 to 1982, the decadal
18 hydrograph is unimodal. A few individual years present a bi-modal shape, but these are too
19 few to influence the decadal mean. In any case the *Red flood* level never exceeds the *Guinean*
20 *flood* in these early decades. The last decade (2003-2012) bi-modal hydrograph shape reflects
21 the increase in intensity and frequency of the annual bi-modal regime and the occurrence of
22 the *Red flood* overpassing the *Guinean flood* (2012, Fig. 2b). Based on the total water volume
23 of the *Red flood* two major periods appear, consistent with the annual mean Niamey *Red flood*
24 discharge index (Fig. 5d): (i) 1953 to 1993 characterised by a decrease of the decadal mean
25 volume during the rainy season (from 7.3 km³ in 1953-1962 to 5.1 km³ in 1983-1992) and
26 (ii) 1993 to 2012 characterised by a steady increase towards the highest values of the whole
27 period (from 7 km³ in 1993-2002 decade to 8.9 km³ in 2003-2012). As previously
28 highlighted in Fig. 5d, the recent *Red flood* (since the 1990s) is higher than during the wettest
29 decades.

30 The simulation reproduces well the unimodal shape of the 1973-1982 hydrograph (Fig. 9).
31 The daily discharge distributions are close to the observation (Fig. 10) for this decade, even

1 though relatively to the other decades (Fig 11) 1973-1982 is too high compared to the
2 observations. In Fig. 11a for observations, the 1983-1992 discharge exceeds 1973-1982
3 discharge, while it is the opposite for the simulations (Fig. 11b).

4 The most striking feature in Figures 9, 10 and 11 is the overestimation of the discharge for the
5 wettest and early decades 1953-1962 and 1963-1972, where the simulations produce too
6 much runoff. For these wet decades, the discharge overestimation leads to an increase of the
7 *Red flood* and a reinforcement of the bi-modal shape of the decadal hydrograph (Fig. 9b),
8 contrary to observations. The high rain rates over the area during the wet decades leads to
9 enhanced runoff and high discharge during the *Red flood*, whereas in the observations the *Red*
10 *flood* values are low during these decades. The *Red flood* decadal mean volume values
11 confirm the strong over estimation for the early decades (Table 2).

12 The present surface conditions (low vegetation cover and high proportion of bare soil) and
13 drainage area, lead to high runoff and local contribution. With these conditions simulations
14 agree with the observed trends in *Red flood* occurrence and intensity between the 1970s-
15 1980s decades and the present period. The rainfall seems to be the main driver of the
16 hydrological changes from the 1970s to the 2010s. For earlier decades (1950s and 1960s) the
17 *Red flood* is highly overestimated, variation in rainfall alone could not explain the changes
18 between wet period and more recent years. Changes in other drivers need to be investigated to
19 understand the hydrological regime evolution.

20 **4.3 Sensitivity to LULC and drainage area changes**

21 Several authors have reported that the LULC and the drainage network have changed in the
22 study area since the 20th century (Leblanc et al. 2008, Amogu et al 2010, Mamadou et al.
23 2015). In this section we investigate the sensitivity of the simulated *Red flood* discharge to the
24 vegetation cover and to the drainage area to assess their potential role in the observed
25 hydrological changes in Niamey. Precise maps of the vegetation and drainage network
26 evolution between 1953 and 2012 are not available. Therefore this part of the study
27 investigates the impact of these changes based on a simplified representation of what has been
28 reported by previous studies (Leblanc et al. 2008, Amogu et al 2010, Mamadou et al. 2015.)
29 This is illustrated in Fig. 4. Figure 4b mimics the 1950s-1960s basin condition: with more
30 vegetation cover (Sahelian wooded savanna) and a smaller drainage area (without north
31 Gorouol and left bank) than in present days (Fig. 4a).

1 Three model configurations are used in this section: (i) standard set up with present condition
2 (SC), (ii) maximum vegetalized condition with a reduce drainage area (VCRD), (iii) and an
3 intermediate situation with maximum vegetalized condition and entire drainage area (VC).

4 The discharges simulated for the decades 1953-1962 and 1963-1972, with the three
5 configurations above are analysed in Fig. 12, and 13. The mean decadal hydrograph for the
6 1953-1962 decade (Fig. 12) displays a marked peak during the *Red flood*, whatever the
7 configuration. However the peak is lower, and closer to the observations (Fig. 9a) for the
8 simulations based on a more vegetated basin, and even lower when the drainage area is
9 reduced. The same effect is observed for the 1963-1972 period.

10 The same behaviour is found for the overall 1953-1962 and 1963-1972 decades, as displayed
11 in the quantile-quantile plots in Fig. 13. Changing the LULC and drainage area improves the
12 daily distribution of the discharge and its relative position compared to the 1983-2012 period.
13 However, unlike for observations (Fig 11a) the Red floods simulated in the 1950s-1960s are
14 still exceeding the Red floods of recent decades (Fig 13c).

15 Some of the remaining positive bias in the VCRD simulation is due to the limits of the ISBA-
16 TRIP model, which is not able to reproduce the loss between Ansongo and Niamey. The
17 coarse resolution of the model and its simple representation of the vegetation cover and the
18 drainage systems are also limitations. Crops or specific Sahelian ecosystems (as in tiger bush,
19 Seghieri et al. 1994, Galle et al. 1999) are not represented explicitly in the present
20 configuration. The complex hydrological behaviour of the temporary tributaries (koris) and
21 their evolution within the season, when heavy rainfall may create new water path-ways is not
22 reproduced with a global model as ISBA-TRIP.

23

24 **5 Conclusion**

25 This paper analyses hydrological changes in the Sahel region since the 1950s with a focus on
26 the middle Niger river in the vicinity of Niamey where floods have increased drastically. The
27 study focuses on the Ansongo-Niamey reach basin where the *Red flood*, that caused many
28 damages in the last decade, is generated. The rainfall over the studied area has followed the
29 general trend that Sahel has overcome between 1953 and 2012: a wet period during 1950s and
30 1960s, a long drought during 1970s and 1980s, and a recent partial recovery of annual
31 rainfall. The intensity of the *Red flood* in Niamey is influenced by the upper Niger flow

1 arriving in Ansongo and by “local” runoff produced in the sub-basin between Ansongo and
2 Niamey. Changes in the *Red flood* signal over the last 60 years are explained by the changes
3 in both components which have been analysed based on standard indexes. The upper Niger
4 contribution has followed the climatic trend. The corresponding index is positive during the
5 1950s-1960s negative during the droughts of the 1970s-1980s, and varies around 0 since the
6 1990s. The local runoff contribution has been continuously increasing over the 1953-2012
7 period, which is paradoxical given the rainfall signal. This double influence results in a
8 progressive increase of the *Red flood* since the 1980s, and paradoxically the *Red flood* has
9 been higher in the last decade than in the wettest decades of the series.

10 This study provides a better understanding of the roles of rainfall and surface conditions
11 (LULC and drainage area) in these observed changes, thanks to hydrological simulations. The
12 simulations based on the current surface conditions are able to reproduce the observed trend
13 in *Red flood* occurrence and intensity since the 1980s. This has been verified with three
14 independent rainfall data sets, which provide similar annual rainfall accumulations over the
15 domain but with marked differences at smaller scales. This result implies that rainfall inter-
16 annual variability is the main driver for the changes observed since the early 1980s: the
17 hydrograph has become bi-modal and the *Red flood* is intensifying. The simulation results
18 since 1953 (only one rainfall product available) reveals that LULC and drainage area changes
19 should be considered. Increasing the vegetation cover and reducing the drainage area
20 decreases the runoff production in the model and simulates discharges closer to the
21 observations 1950s and 1960s. This result implies that changes in the environmental
22 conditions are responsible for the change in hydrological behaviour between the 1950s-1960s
23 decades and the 1970s to present period. The scenario which emerges from these results is the
24 following: in 1950s and 1960s surface conditions, with more woody area and bare soil than in
25 the present days, limited the runoff and thus the local contribution to the *Red flood* despite the
26 high rainfall amounts. Changes in surface conditions (because of climatic variations and
27 anthropic pressure) during 1970s and 1980s have increased the runoff coefficient as already
28 suggested by many authors (Amani and Nguetora 2002, Mahé et al. 2003, Amogu et al. 2010,
29 Descroix et al. 2013, Aich et al. 2015). This led to an increased local contribution to the *Red*
30 *flood* in spite of the rainfall deficit. This new surface conditions result in an enhanced
31 sensitivity of the hydrological response to rainfall variability, because runoff has increased
32 and surface water propagates relatively fast on bare or poorly vegetated soils. Accordingly,
33 since the 1990s, the rainfall “recovery” is enhancing the local runoff production and conducts

1 to a dramatic increase of the *Red flood*. The *Red flood* is also well separated in time from the
2 *Guinean flood*, exceeds it, and has reached the highest level ever recorded. Climate variability
3 with its consequences on the rainfall regime, and LULC changes have both played a role, in
4 turn, in the recent flood risk increase in Niamey. Whether climate/rainfall variability or LULC
5 is the dominant factor depends on the period considered.

6 This study brings more light on the temporality of the different driver role, compared to
7 previous studies (Seguis et al. 2004, D'Orgeval and Polcher, 2008, Aich et al., 2015).

8 More work could be done to analyse the exact timing of the changes. The model used here is
9 relatively coarse in resolution, the physics is simplified and does not represent all the
10 complexity of the vegetation-hydrology interaction. Uncertainties in the rainfall forcing and
11 the discharge data is also limiting. Further effort should be done to understand the role of
12 rainfall in the recent increase of the Red flood intensity. Has some specific changes in the
13 rainfall regime contributed to the increased flood risk (increase in the frequency or intensity
14 of extreme events, changes in the dry/wet spells, etc...)? High-resolution rainfall products,
15 models and LULC changes maps are needed to investigate these questions at the relevant
16 scales. Effort should also be done to better understand the drainage area changes and integrate
17 a more realistic representation of the temporary rivers (Koris) and of the endoreic areas, in the
18 hydrological modelling.

19

1 **Appendix A: Rainfall products analysis**

2 The 3 long-term rainfall data set used in the present study have been evaluated against a dense
3 network of gauges. The network is one of the 3 instrumented sites of the AMMA-CATCH
4 observatory system (African Monsoon Multidisciplinary Analysis - CATCH standing for
5 Couplage de l'Atmosphère Tropicale et du Cycle Hydrologique in French, Lebel et al. 2010).
6 It is located in the region of Niamey. The site covers an area of $1^{\circ} \times 1^{\circ}$ (centred at 2.5°E and
7 13.5°N) and monitors the rainfall since 1990 with a dense gauge network (between 40 and 50
8 gauges). This high resolution network was already used as a reference to compare and
9 validate satellite rainfall products (Roca et al. 2010, Gosset et al. 2013, Kirstetter et al. 2012).
10 The rain gauges produce 5min punctual rainfall series which are interpolated to a $0.25^{\circ}\text{-}3\text{h}$
11 grid by Langrangian kriging (Vischel et al. 2011). This ground reference is referred to as
12 "KRIG DENSE" hereafter.

13 Figure A1 compares the 3 rainfall estimates and the ground reference KRIG DENSE. The
14 comparison is carried out on four pixels of 0.5° at a daily time step between 1990 and 2012 for
15 the雨iest months (June, July, August and September). The interannual series of rainfall
16 accumulation is satisfactory for all 3 products, but KRIG is closer to the reference ($r^2 0.85$)
17 than PERSIANN-CDR ($r^2 0.7$) and CPC ($r^2 0.68$). KRIG and PERSIANN-CDR tend to
18 smooth the rainfall fields in time, with a low daily conditional mean rainfall (Fig. A1b) and a
19 lot of rainy days (Fig. A1c). Both KRIG and PERSIANN-CDR reproduce well the rainfall
20 extension seen by the reference between 1990 and 2005 but KRIG overestimates the spatial
21 extension in the last 5 years (this is attributed to the reduce number of gauges in the network).
22 CPC follows the tendency observed with the reference but has the greatest interannual
23 variability and tends to underestimate the rainfall events extension. As already highlighted in
24 several studies (Roca et al. 2010, Gosset et al 2013, Casse et al. 2015), rainfall products with
25 similar annual rainfall accumulation, may exhibit large differences in the spatial, temporal and
26 intensity distribution of rainfall. These differences impact the hydrological simulations (Casse
27 et al. 2015).

28

1 **Acknowledgements**

2 We warmly thank the Niger Basin Authority (ABN), for providing the Niger River discharge
3 data and for their collaboration. We would like also to thank all the teams that provided the
4 various rainfall data sets online. We also are grateful to L. Gal for her precious help and
5 advice for the maps. This work has been co-funded by the French Centre National d'Etudes
6 spatiales (CNES) and the Midi-Pyrénées region. It was also partly supported by the French
7 national programme EC2CO-LEFE “Evolution récente de l'aléa hydro-climatique au Sahel:
8 détection et éléments d'attribution”.

9

1 **References**

2 Aich, V., Liersch, S., Vetter, T., Andersson, J., Müller, E. and Hattermann, F.: Climate or
3 Land Use?—Attribution of Changes in River Flooding in the Sahel Zone, *Water*, 7(6), 2796–
4 2820, doi:10.3390/w7062796, 2015.

5 Albergel, J.: Sécheresse, désertification et ressources en eau de surface - Application aux
6 petits bassins du Burkina Faso, in *The Influence of Climate Change and Climatic Variability*
7 on the Hydrologic Regime and Water Resources

8 PUBLICATION, Vancouver., 1987.

9 Amani, A. and Nguetora, M.: Evidence d'une modification du régime hydrologique du fleuve
10 Niger à Niamey, in *4th FRIEND 2002 - Regional Hydrology: Bridging the Gap between*
11 *Research and practice*, vol. 274, pp. 449–456, IAHS PUBLICATION, Cape Town, South
12 Africa., 2002.

13 D'Amato, N. and Lebel, T.: On the Characteristics of the rainfall eveents in the Sahel with a
14 view to the analysis of climatic variability, *Int. J. Climatol.*, 18, 955–974, 1998.

15 Amogu, O., Descroix, L., Yéro, K. S., Le Breton, E., Mamadou, I., Ali, A., Vischel, T.,
16 Bader, J.-C., Moussa, I. B., Gautier, E., Boubkraoui, S. and Belleudy, P.: Increasing River
17 Flows in the Sahel?, *Water*, 2(2), 170–199, doi:10.3390/w2020170, 2010.

18 Ashouri, H., Hsu, K.-L., Sorooshian, S., Braithwaite, D. K., Knapp, K. R., Cecil, L. D.,
19 Nelson, B. R. and Prat, O. P.: PERSIANN-CDR: Daily Precipitation Climate Data Record
20 from Multisatellite Observations for Hydrological and Climate Studies, *B. Am. Meteorol.*
21 Soc., 96(1), 69–83, doi:10.1175/BAMS-D-13-00068.1, 2015.

22 Le Barbé, L. and Lebel, T.: Rainfall climatology of the HAPEX-Sahel region during the years
23 1950-1990, *J. Hydrol.*, 188-189, 43–73, 1997.

24 Le Barbé, L., Lebel, T. and Tapsoba, D.: Rainfall variability in West Africa during the years
25 1950-90, *J. Climate.*, 15(2), 187–202, 2002.

26 Boone, A., Calvet, J.-C. and Noilhan, J.: Inclusion of a third soil layer in a land surface
27 scheme using the force-restore method, *J. Appl. Meteorol.*, 38(11), 1611–1630, 1999.

28 Briquet, J. P., Mahé, G., Bamba, F. and Olivry, J. C.: Changements climatiques recents et
29 modification du régime hydrologique du fleuve Niger Koulikoro (Mali), in *L'hydrologie*
30 *tropicale : géoscience et outil pour le développement*, vol. 238, pp. 157–166, IAHS
31 PUBLICATION, Paris, 1996.

32 Camberlin, P., Beltrando, G., Fontaine, B. and Richard, Y.: Pluviométrie et crises climatiques
33 en Afrique Tropicale : changements durables ou fluctuations interannuelles ?, *Histoire et*
34 *Géographes*, (379), 263–273, 2002.

35 Casenave, A. and Valentin, C.: A runoff capability classification system based on surface
36 features criteria in semi-arid areas of West Africa, *J. Hydrol.*, 130, 231–249, 1992.

37 Casse, C. and Gosset, M.: Analysis of hydrological changes and flood increase in Niamey
38 based on the PERSIANN-CDR satellite rainfall estimate and hydrological simulations over
39 the 1983–2013 period, *Proceedings of the International Association of Hydrological Sciences*,
40 370, 117–123, doi:10.5194/piahs-370-117-2015, 2015.

1 Casse, C., Gosset, M., Peugeot, C., Pedinotti, V., Boone, A., Tanimoun, B. A. and Decharme,
2 B.: Potential of satellite rainfall products to predict Niger River flood events in Niamey,
3 Atmos. Res., 163, 162–176, doi:10.1016/j.atmosres.2015.01.010, 2015.

4 Chen, M., Shi, W., Xie, P., Silva, V. B. S., Kousky, V. E., Wayne Higgins, R. and Janowiak,
5 J. E.: Assessing objective techniques for gauge-based analyses of global daily precipitation, J.
6 Geophys. Res., 113, D04110, doi:10.1029/2007JD009132, 2008.

7 Collinet, J. and Valentin, C.: Analyse des différents facteurs intervenant sur
8 l'hydrodynamique superficielle, Nouvelle perspectives - Applications agronomiques,
9 ORSTOM, Centre d'Adiopodoume, B.P V-51 Abidjan (Côte d'Ivoire), 1979.

10 Dai, A., Lamb, P. J., Trenberth, K. E., Hulme, M., Jones, P. D. and Xie, P.: The recent Sahel
11 drought is real, Int. J. Climatol., 24(11), 1323–1331, doi:10.1002/joc.1083, 2004.

12 Decharme, B. and Douville, H.: Introduction of a sub-grid hydrology in the ISBA land surface
13 model, Clim. Dynam., 26(1), 65–78, doi:10.1007/s00382-005-0059-7, 2005.

14 Decharme, B. and Douville, H.: Global validation of the ISBA sub-grid hydrology, Clim.
15 Dynam., 29(1), 21–37, doi:10.1007/s00382-006-0216-7, 2007.

16 Decharme, B., Douville, H., Boone, A., Habets, F. and Noilhan, J.: Impact of an exponential
17 profile of saturated hydraulic conductivity within the ISBA LSM: Simulations over the Rhône
18 basin., J. Hydrometeorol., 7(1), 2006.

19 Desconnets, J. C., Taupin, J. D., Lebel, T. and Leduc, C.: Hydrology of the HAPEX-Sahel
20 Central Super-site: surface water drainage and aquifer recharge through the pool systems, J.
21 Hydrol., 188-189, 155–178, 1997.

22 Descroix, L., Mahé, G., Lebel, T., Favreau, G., Galle, S., Gautier, E., Olivry, J.-C., Albergel,
23 J., Amogu, O., Cappelaere, B., Dessouassi, R., Diedhiou, A., Le Breton, E., Mamadou, I. and
24 Sighomnou, D.: Spatio-temporal variability of hydrological regimes around the boundaries
25 between Sahelian and Sudanian areas of West Africa: A synthesis, J. Hydrol., 375(1-2), 90–
26 102, doi:10.1016/j.jhydrol.2008.12.012, 2009.

27 Descroix, L., Genthon, P., Amogu, O., Rajot, J.-L., Sighomnou, D. and Vauclin, M.: Change
28 in Sahelian Rivers hydrograph: The case of recent red floods of the Niger River in the Niamey
29 region, Global Planet. Change, 98-99, 18–30, doi:10.1016/j.gloplacha.2012.07.009, 2012.

30 Descroix, L., Niang, A. D., Dacosta, H., Panthou, G., Quantin, G. and Diedhiou, A.:
31 Evolution des pluies de cumul élevé et recrudescence des crues depuis 1951 dans le bassin du
32 Niger Moyen (Sahel), Climatologie, 10, 37–50, 2013.

33 Eldridge, R. H.: A synoptic study of West African disturbance lines, Q. J. Roy. Meteor. Soc.,
34 83(357), 303–314, 1957.

35 Galle, S., Ehrmann, M. and Peugeot, C.: Water balance in a banded vegetation pattern: a case
36 study of tiger bush in western Niger, Catena, 37(1), 197–216, 1999.

37 Gandin, L. S., Objective Analysis of Meteorological Fields. Leningrad, Gidromet; Translated
38 from Russian, Jerusalem, Israel Program for Scientific Translations, 1965, 242pp, 1965.

1 Gardelle, J., Hiernaux, P., Kergoat, L. and Grippa, M.: Less rain, more water in ponds: a
2 remote sensing study of the dynamics of surface water from 1950 to present in pastoral Sahel
3 (Gourma region, Mali), *Hydrol. Earth Syst. Sc.*, 14(2), 309–324, 2010.

4 Gosset, M., Viarre, J., Quantin, G. and Alcoba, M.: Evaluation of several rainfall products
5 used for hydrological applications over West Africa using two high-resolution gauge
6 networks, *Q. J. Roy. Meteor. Soc.*, 139(673), 923–940, doi:10.1002/qj.2130, 2013.

7 Hiernaux, P. and Le Houérou, H. N.: Les parcours du Sahel, *Sécheresse*, 17(1-2), 51–71,
8 2006.

9 L’Hote, Y., Mahé, G., Somé, B. and Triboulet, J. P.: Analysis of a Sahelian annual rainfall
10 index from 1896 to 2000; the drought continues, *Hydrolog. Sci. J.*, 47(4), 563–572, 2002.

11 Houze, R. A.: Cloud dynamics, *International Geophysics Series*, 53, Academic Press Inc., San
12 Diego, 1993.

13 Huffman, G. J., Adler, R. F., Arkin, P., Chang, A., Ferraro, R., Gruber, A., Janowiak, J.,
14 McNab, A., Rudolf, B. and Schneider, U.: The Global Precipitation Climatology Project
15 (GPCP) Combined Precipitation Dataset, *B. Am. Meteorol. Soc.*, 78(1), 5–20, 1997.

16 Huffman, G. J., Adler, R. F., Bolvin, D. T. and Gu, G.: Improving the global precipitation
17 record: GPCP Version 2.1, *Geophy. Res. Lett.*, 36(17), L17808, doi:10.1029/2009GL040000,
18 2009.

19 Kirstetter, P.-E., Viltard, N. and Gosset, M.: An error model for instantaneous satellite rainfall
20 estimates: evaluation of BRAIN-TMI over West Africa, *Q. J. Roy. Meteor. Soc.*, 139(673),
21 894–911, doi:10.1002/qj.1964, 2012.

22 Lamb, P. J.: Persistence of Subsaharan drough, *Nature*, 299, 46–48, 1982.

23 Laurent, H., d’Amato, N. and Lebel, T.: How important is the contribution of the mesoscale
24 convective complexes to the Sahelian rainfall?, *Phys. Chem. Earth*, 23(5), 629–633, 1998.

25 Lebel, T. and Ali, A.: Recent trends in the Central and Western Sahel rainfall regime (1990–
26 2007), *J. Hydrol.*, 375, 1-2, 52–64, doi:10.1016/j.jhydrol.2008.11.030, 2009.

27 Lebel, T., Diedhiou, A. and Laurent, H.: Seasonal cycle and interannual variability of the
28 Sahelian rainfall at hydrological scales, *J. Geophys. Res.*, 108, 8, 8389,
29 doi:10.1029/2001JD001580, 2003.

30 Lebel, T., Parker, D. J., Flamant, C., Bourlès, B., Marticorena, B., Mougin, E., Peugeot, C.,
31 Diedhiou, A., Haywood, J. M., Ngamini, J. B., Polcher, J., Redelsperger, J.-L. and Thorncroft,
32 C. D.: The AMMA field campaigns: multiscale and multidisciplinary observations in the
33 West African region, *Q. J. Roy. Meteor. Soc.*, 136, 1, 8–33, doi:10.1002/qj.486, 2010.

34 Leblanc, M. J., Favreau, G., Massuel, S., Tweed, S. O., Loireau, M. and Cappelaere, B.: Land
35 clearance and hydrological change in the Sahel: SW Niger, *Global Planet. Change*, 61(3-4),
36 135–150, doi:10.1016/j.gloplacha.2007.08.011, 2008.

37 Leduc, C., Favreau, G. and Schroeter, P.: Long-term rise in a Sahelian water-table: The
38 Continental Terminal in south-west Niger, *J. Hydrol.*, 243(1), 43–54, 2001.

1 Li, K. Y., Coe, M. T., Ramankutty, N. and De Jong, R.: Modeling the hydrological impact of
2 land-use change in West Africa, *J. Hydrol.*, 337(3-4), 258–268,
3 doi:10.1016/j.jhydrol.2007.01.038, 2007.

4 Mahé, G.: Surface/groundwater interactions in the Bani and Nakambe rivers, tributaries of the
5 Niger and Volta basins, West Africa, *Hydrolog. Sci. J.*, 54(4), 704–712,
6 doi:10.1623/hysj.54.4.704, 2009.

7 Mahé, G. and Paturel, J.-E.: 1896–2006 Sahelian annual rainfall variability and runoff
8 increase of Sahelian Rivers, *Comptes Rendus Geoscience*, 341(7), 538–546,
9 doi:10.1016/j.crte.2009.05.002, 2009.

10 Mahé, G., Olivry, J.-C., Dessouassi, R., Orange, D., Bamba, F. and Servat, E.: Relations eaux
11 de surface–eaux souterraines d'une rivière tropicale au Mali, *Comptes Rendus de l'Académie
12 des Sciences-Series IIA-Earth and Planetary Science*, 330(10), 689–692, 2000.

13 Mahé, G., Leduc, C., Amani, A., Paturel, J. E., Girard, S., Servat, E. and Dezetter, A.:
14 Augmentation récente du ruissellement de surface en région soudano-sahélienne et impact sur
15 les ressources en eau, in *Hydrology of the Mediterranean and Semiarid Region*, vol. 278, pp.
16 215–222, IAHS PUBLICATION, Montpellier, 2003.

17 Mahé, G., Paturel, J.-E., Servat, E., Conway, D. and Dezetter, A.: The impact of land use
18 change on soil water holding capacity and river flow modelling in the Nakambe River,
19 Burkina-Faso, *J. Hydrol.*, 300(1-4), 33–43, doi:10.1016/j.jhydrol.2004.04.028, 2005.

20 Mamadou, I., Gautier, E., Descroix, L., Noma, I., Bouzou Moussa, I., Faran Maiga, O.,
21 Genthon, P., Amogu, O., Malam Abdou, M. and Vandervaere, J.-P.: Exorheism growth as an
22 explanation of increasing flooding in the Sahel, *Catena*, 131, 130–139,
23 doi:10.1016/j.catena.2015.03.017, 2015.

24 Masson, V., Champeaux, J.-L., Chauvin, F., Meriguet, C. and Lacaze, R.: A global database
25 of land surface parameters at 1-km resolution in meteorological and climate models, *J.
26 Climate*, 16(9), 1261–1282, 2003.

27 Masson, V., Le Moigne, P., Martin, E., Faroux, S., Alias, A., Alkama, R., Belamari, S.,
28 Barbu, A., Boone, A., Bouyssel, F., and others: the SURFEXv7. 2 land and ocean surface
29 platform for coupled or o_ine simulation of Earth surface variables and fluxes, *Geosci. Model
30 Dev.*, 6, 929-960, doi:10.5194/gmd-6-929-2013, 2013.

31 Mathon, V. and Laurent, H.: Life cycle of Sahelian mesoscale convective cloud systems, *Q. J.
32 Roy. Meteor. Soc.*, 127(572), 377–406, 2001.

33 Mathon, V., Laurent, H. and Lebel, T.: Mesoscale convective system rainfall in the Sahel, *J.
34 Appl. Meteorol.*, 41(11), 1081–1092, 2002.

35 Millot, J. A.: Les crues du Niger, *Annales de Géographie*, 22(121), 68–93,
36 doi:10.3406/geo.1913.8385, 1913.

37 Narisma, G. T., Foley, J. A., Licker, R. and Ramankutty, N.: Abrupt changes in rainfall
38 during the twentieth century, *Geophys. Res. Lett.*, 34, 6, L06710,
39 doi:10.1029/2006GL028628, 2007.

1 Nicholson, S. E., Some, B. and Kone, B.: An analysis of recent rainfall conditions in West
2 Africa, including the rainy seasons of the 1997 El Niño and the 1998 La Niña years, *J.*
3 *Climate*, 13(14), 2628–2640, 2000.

4 Nka, B. N., Oudin, L., Karambiri, H., Paturel, J. E. and Ribstein, P.: Trends in West African
5 floods: a comparative analysis with rainfall and vegetation indices, *Hydrol. Earth Syst. Sc.*,
6 12(5), 5083–5121, doi:10.5194/hessd-12-5083-2015, 2015.

7 Noilhan, J. and Planton, S.: A Simple Parametrization of Land Surface Processes for
8 Meteorological Models, *Mon. Weather Rev.*, 117, doi : [http://dx.doi.org/10.1175/1520-0493\(1989\)117<0536:ASPOLS>2.0.CO;2](http://dx.doi.org/10.1175/1520-0493(1989)117<0536:ASPOLS>2.0.CO;2), 1989.

10 D'Orgeval, T. and Polcher, J.: Impacts of precipitation events and land-use changes on West
11 African river discharges during the years 1951–2000, *Clim. Dynamics*, 31(2-3), 249–262,
12 doi:10.1007/s00382-007-0350-x, 2008.

13 Panthou, G., Vischel, T. and Lebel, T.: Recent trends in the regime of extreme rainfall in the
14 Central Sahel, *Int. J. Climatol.*, 34(15), 3998–4006, doi:10.1002/joc.3984, 2014.

15 Paturel, J.-E., Diawara, A., Kong, A., Siou, L., Talin, E., Ferry, L., Mahé, G., Dezetter, A.,
16 Muther, N., Martin, D. and others: Caractérisation de la sécheresse hydropluviométrique du
17 Bani, principal affluent du fleuve Niger au Mali, in *Global Change: Facing Risks and Threats*
18 to Water Resources, IAHS PUBLICATION, 661–667, Fez, 2010.

19 Pedinotti, V., Boone, A., Decharme, B., Crétaux, J. F., Mognard, N., Panthou, G. and Papa,
20 F.: Characterization of the hydrological functioning of the Niger basin using the ISBA-TRIP
21 model, *Hydrol. Earth Syst. Sc.*, 8(5), 9173–9227, doi:10.5194/hessd-8-9173-2011, 2012.

22 Peltier, R., Bertrand, A., Lawali, E. M., Madon, G. and Montagne, P.: Marchés ruraux de
23 bois-énergie ay Sahel, Bois et Forêts des Tropiques, 245, 3^{ème} Trimestre, 1995.

24 Pradé, M.: Fleuves et rivières, *Les Études rhodaniennes*, 10, 1-2, 97–100, 1934.

25 Roca, R., Chambon, P., Jobard, I., Kirstetter, P.-E., Gosset, M. and Bergès, J.-C.: Comparing
26 Satellite and Surface Rainfall Products over West Africa at Meteorologically Relevant Scales
27 during the AMMA Campaign Using Error Estimates, *J. Appl. Meteorol. Clim.*, 49(4), 715–
28 731, doi:10.1175/2009JAMC2318.1, 2010.

29 Rowell, D. P. and Milford, J. R.: On the Generation of African Squall Lines, *J. Climate*, 6,
30 1181–1193, 1993.

31 Seghieri, J., Galle, S. and Rajot, J. L.: La brousse tigrée dans le Sahel Nigérien : étude de la
32 cofluctuation du stock hydrique et de la végétation annuelle, X^e journées hydrologiques, pp.
33 123–141, ORSTOM., 1994.

34 Seguis, L., Cappelaere, B., Milesi, G., Peugeot, C., Massuel, S. and Favreau, G.: Simulated
35 impacts of climate change and land-clearing on runoff from a small Sahelian catchment,
36 *Hydrol. Process.*, 18(17), 3401–3413, 2004.

37 Sighomnou, D., Descroix, L., Mahe, G., Moussa, I. B., Gautier, E., Mamadou, I.,
38 Vandervaere, J.-P., Bachir, T., Coulibaly, B., Rajot, J.-L., Issa, O. M., Dessay, N., Delaître,
39 E., Maiga, O. F., Diedhiou, A., Panthou, G., Vischel, T., Yacouba, H., Karambiri, H., Paturel,
40 J. E., Diello, P., Mougin, E., Kergoat, L. and Hiernaux, P.: La crue de 2012 à Niamey : un

1 paroxysme du paradoxe du Sahel?, Sécheresse, 24(1), 3–13, doi:10.1684/sec.2013.0370,
2 2013.

3 Sorooshian, S., Hsu, K., Gao, X., Gupta, H. V., Imam, B. and Braithwaite, D.: Evaluation of
4 PERSIANN System Satellite-Based Estimates of Tropical Rainfall, B. Am. Meteorol. Soc.,
5 81(9), 2035–2046, 2000.

6 Valentin, C., Rajot, J.-L. and Mitja, D.: Responses of soil crusting, runoff and erosion to
7 fallowing in the sub-humid and semi-arid regions of West Africa, Agriculture, Ecosystems &
8 Environment, 104(2), 287–302, doi:10.1016/j.agee.2004.01.035, 2004.

9 Vischel, T., Quantin, G., Lebel, T., Viarre, J., Gosset, M., Cazenave, F. and Panthou, G.:
10 Generation of High-Resolution Rain Fields in West Africa: Evaluation of Dynamic
11 Interpolation Methods, J. Hydrometeorol., 12(6), 1465–1482, doi:10.1175/JHM-D-10-
12 05015.1, 2011.

13 Weedon, G. P., Gomes, S., Viterbo, P., Shuttleworth, W. J., Blyth, E., Österle, H., Adam, J.
14 C., Bellouin, N., Boucher, O. and Best, M.: Creation of the WATCH Forcing Data and Its Use
15 to Assess Global and Regional Reference Crop Evaporation over Land during the Twentieth
16 Century, J. Hydrometeorol., 12(5), 823–848, doi:10.1175/2011JHM1369.1, 2011.

17 Weedon, G. P., Balsamo, G., Bellouin, N., Gomes, S., Best, M. J., Viterbo, P.: The WFDEI
18 meteorological forcing data set: WATCH Forcing Data methodology applied to ERA-Interim
19 reanalysis data, Water Resour. Res., 50, 7505–7514, doi: 10.1002/2014WR015638.

20

1 Table 1: Summary of the different rainfall estimate products characteristics.

| | Data | Cover | Temp. Res. | Spa. Res. | Dates | Used period | Agencies | Ref | Web |
|---------------------|----------------------|---------|------------|-----------|--------------|-------------|-----------|----------------------|---|
| KRIG | in-situ | | Daily | 0.5° | 1950-2012 | 1953-2012 | LTHE | Panthou et al., 2014 | |
| CPC | in-situ | Global | Daily | 0.5° | 1979-present | 1983-2012 | NOAA /CPC | Chen et al., 2008 | http://www.cpc.noaa.gov/products/fews/data.html |
| PERSIANN-CDR | satellite in-situ | 60° N-S | Daily | 0.25° | 1983-2013 | 1983-2012 | NOAA | Ashouri et al., 2015 | http://www.ncdc.noaa.gov/cdr/operationalcdrs.html |

2

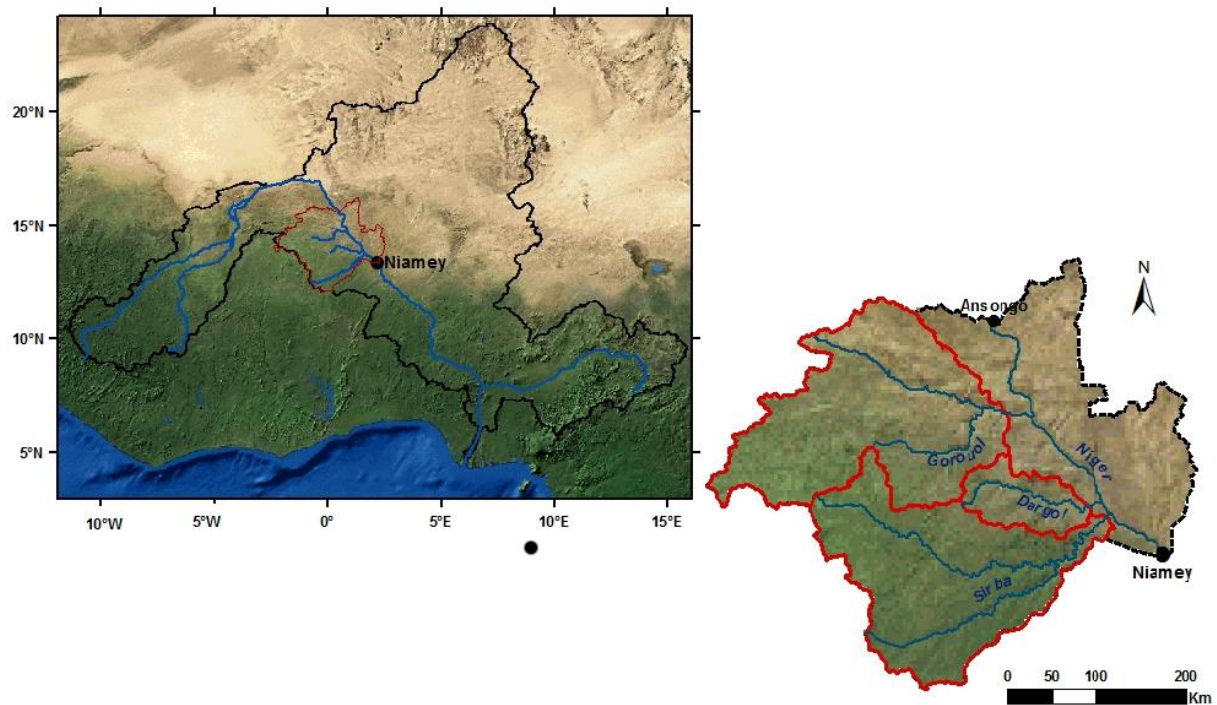
3

1 Table 2: Observed and simulated decadal mean total Red flood volume (in km³), and
 2 difference between observed and simulated values (expressed in observation percentage).

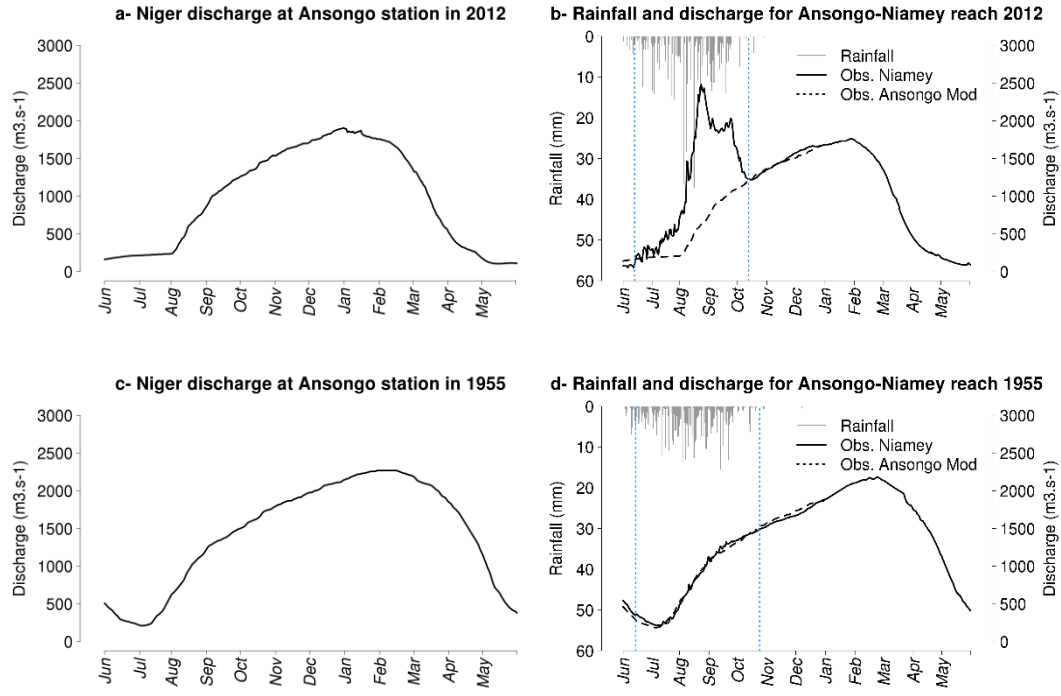
| | 1953-1962 | 1963-1972 | 1973-1982 | 1983-1992 | 1993-2002 | 2003-2012 |
|----------------------------|------------------|------------------|------------------|------------------|------------------|------------------|
| <i>Observation</i> | 7.3 | 6.1 | 5.6 | 5.1 | 7 | 8.9 |
| <i>KRIG</i> | 12.5 | 9.2 | 6.9 | 5.3 | 7.9 | 8.7 |
| | 70% | 50.5% | 23.5% | 4% | 13% | -2% |
| <i>CPC</i> | - | - | - | 6.6 | 8.8 109 | 9.3 109 |
| | - | - | - | 30% | 26.5% | 5% |
| <i>PERSIANN-CDR</i> | - | - | - | 5.4 109 | 8.5 109 | 9.6 109 |
| | - | - | - | 6% | 22% | 7% |

3

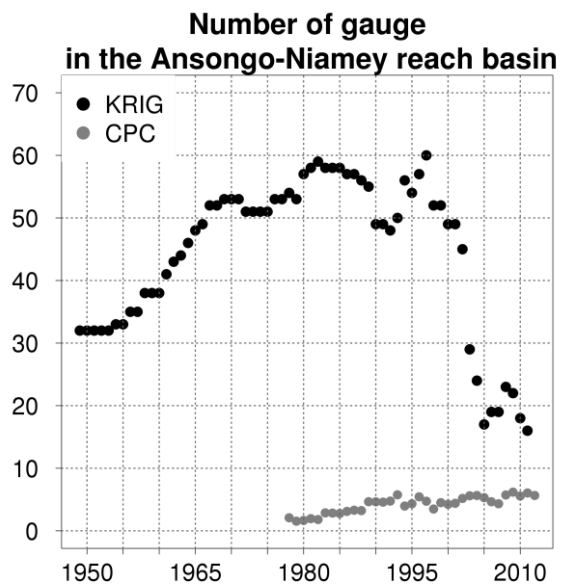
4



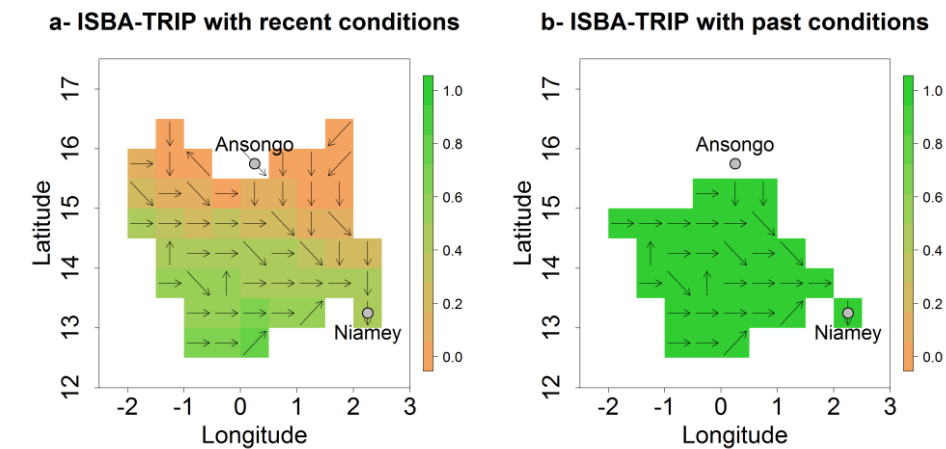
1
2 Figure 1: Map of the Niger basin (top left) and zoom on the Ansongo-Niamey reach basin
3 (bottom right). The red contours on the bottom right plots delineate the 3 main tributaries
4 contributing to the Red flood (C. Casse and L. Gal, based on SIEREM and NOAA data base).
5



1 Figure 2: Discharge of the Niger in Ansongo station in 2012 (a) and 1955 (c) and discharge of
 2 the Niger in Niamey (black line) and Ansongo (dashed line) after morphing (see Sec. 2.3) in
 3 2012 (b) and 1955 (d). The downwards grey bars in b) and d) are the daily rainfall in
 4 Ansongo-Niamey reach basin. The blue vertical lines in b) and d) indicate the beginning and
 5 the end of the Red flood period.
 6
 7



2 Figure 3: Number of rain gauges for the two in-situ rainfall estimates products KRIG (black
3 dots) and CPC (gray dots) on the Ansongo-Niamey reach basin.



1
2
3
4
5

Figure 4: ISBA-TRIP domain implemented on the Ansongo-Niamey reach basin. The color scale represent the vegetation fraction on the area. Green colour and values close to 1 indicate full vegetated cells and brown colour and values close to 0 indicate bare soil.

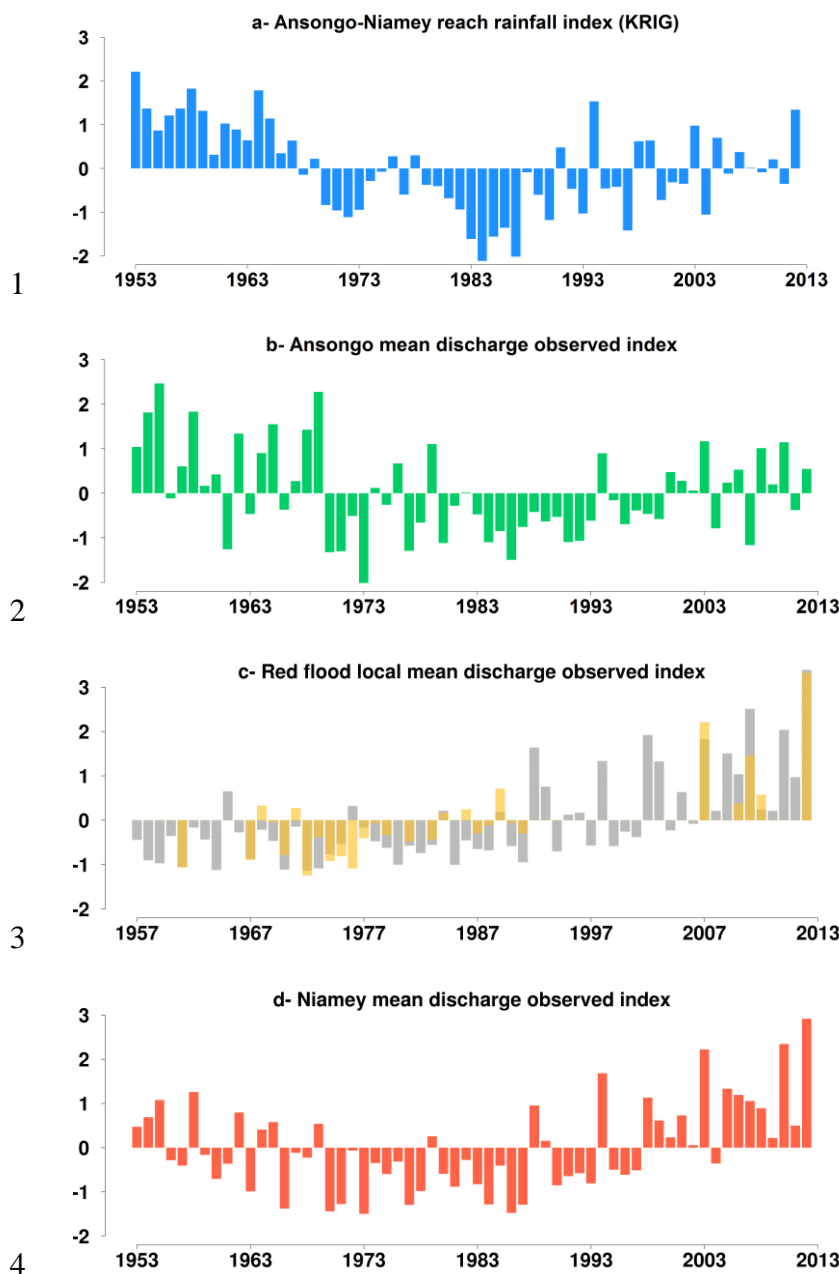
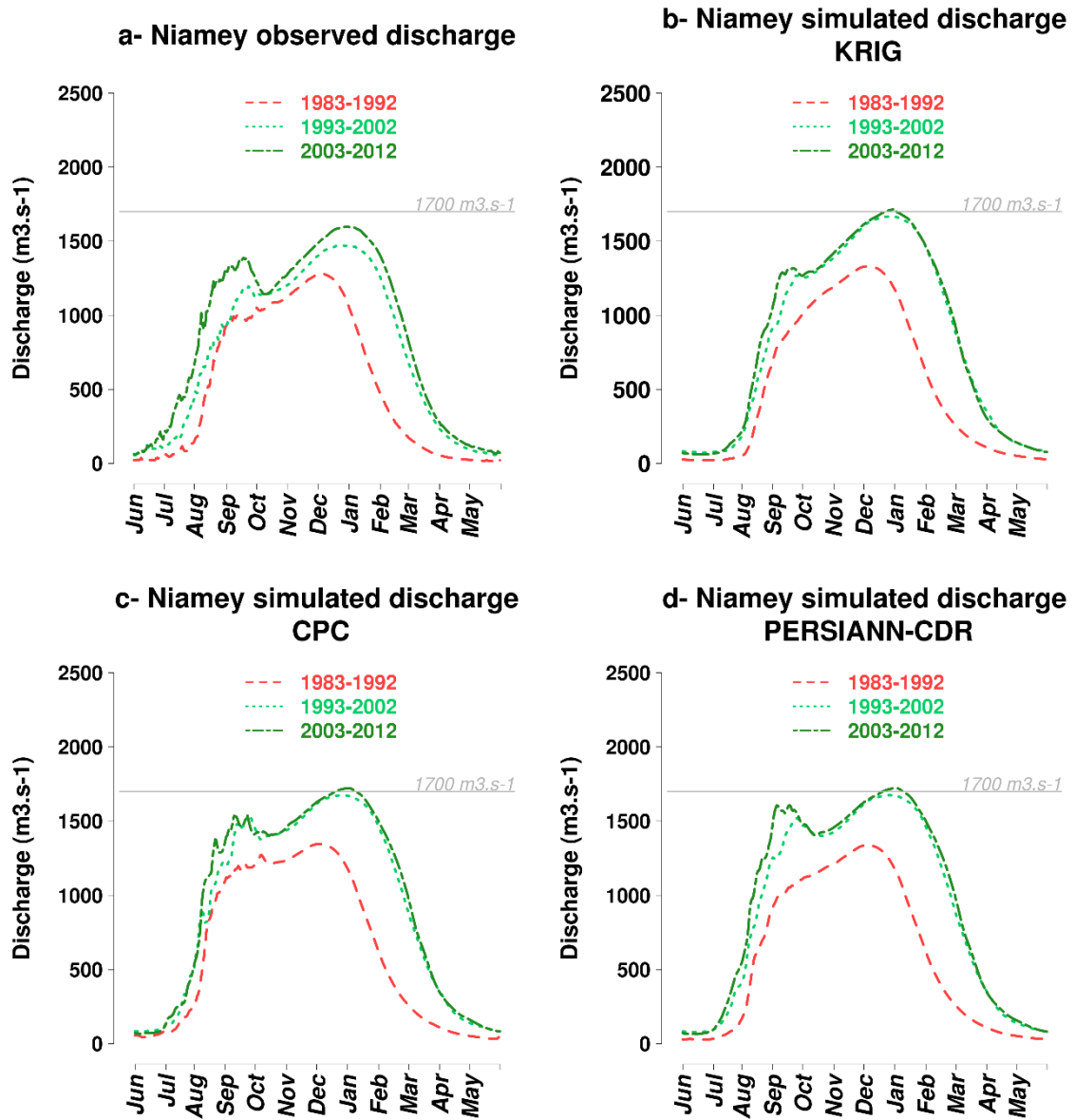
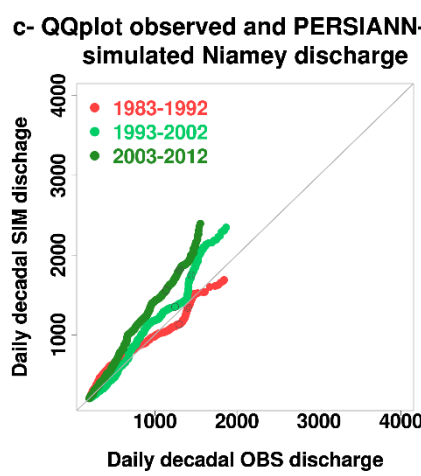
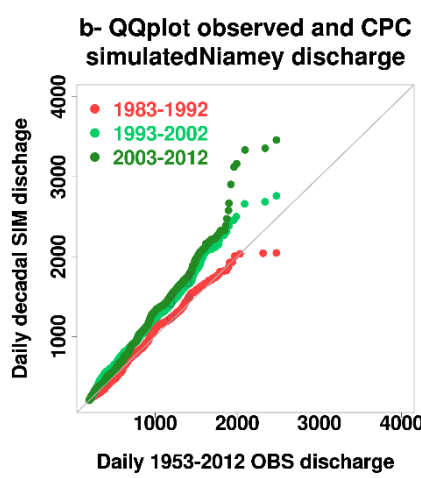
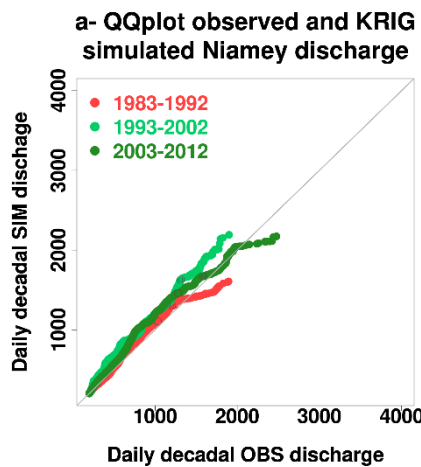


Figure 5: Evolution between 1953 and 2012 of the normalized indexes of: rainfall (a), Red flood period mean discharge in Ansongo (modified after morphing method, see Sec. 2.3) (b), Red flood period mean differential discharge between Ansongo and Niamey (c, grey), Red flood period mean discharge of the 3 right bank tributaries (c, yellow) and Red flood mean discharge Niamey (d).

10

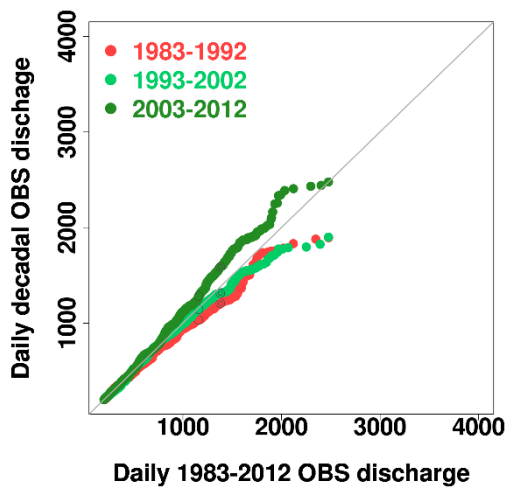


3 Figure 6: Observed and simulated decadal mean Niamey discharge between 1983 and 2012.

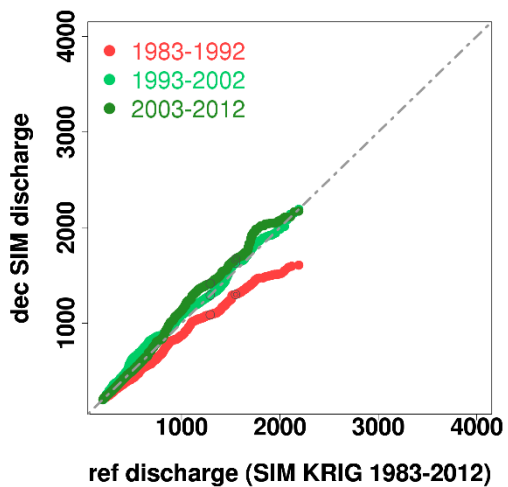


4 Figure 7: Quantile-Quantile plot of the Red flood period distribution of daily discharge of
5 each decade between 1983 and 2012. The x axis is for observations and the y axis for the
6 simulations.

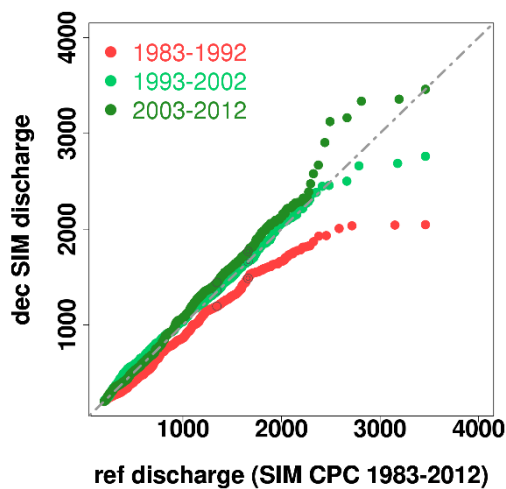
1 a- QQplot observed Niamey discharge



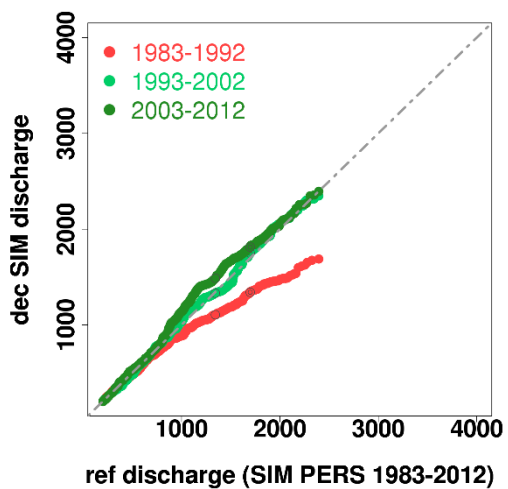
1 b- QQplot discharge Niamey KRIG



2 c- QQplot discharge Niamey CPC

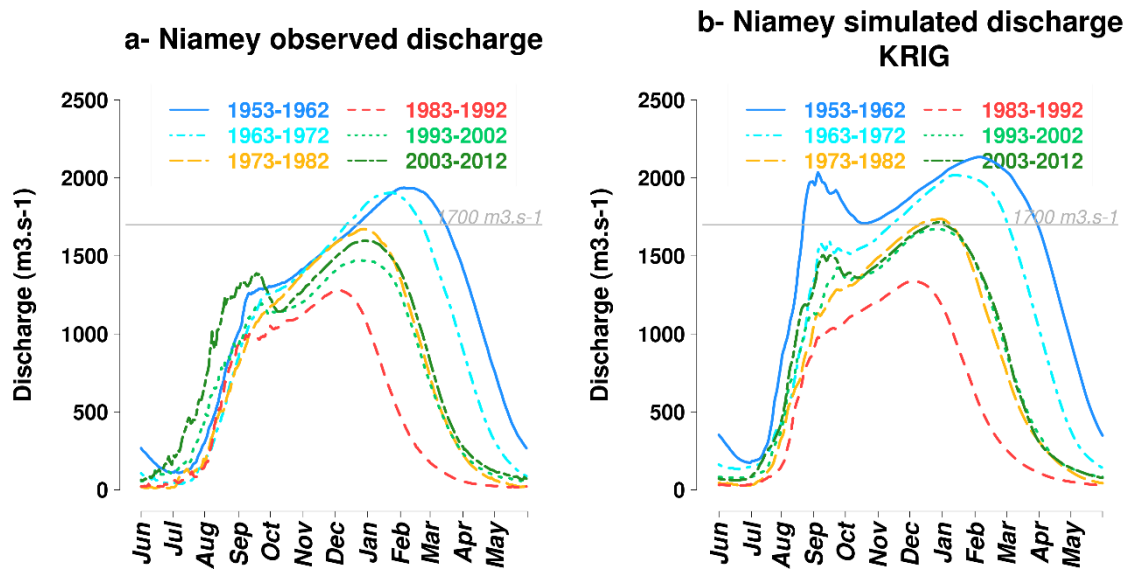


2 d- QQplot discharge Niamey PERSIANN-CDR



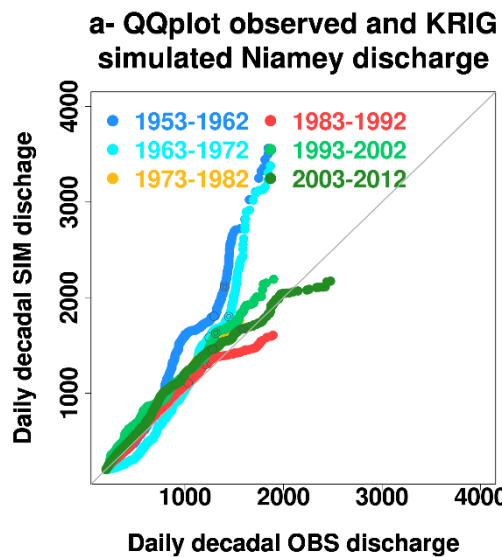
3 Figure 8: Quantile-Quantile plot of the distribution of daily discharge in Niamey (observed in
4 a; simulated in b-c-d) for each decade, the reference (x axis) is the Red flood
5 observed/simulated daily discharge between 1983 and 2012.

6



1 Figure 9: Observed and simulated decadal mean discharge at Niamey station between 1953
2 and 2012.

3

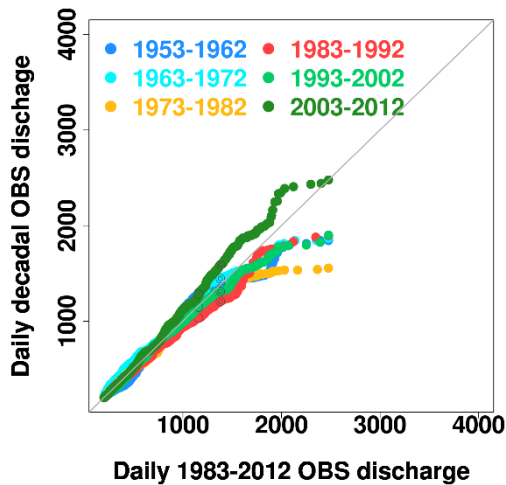


1

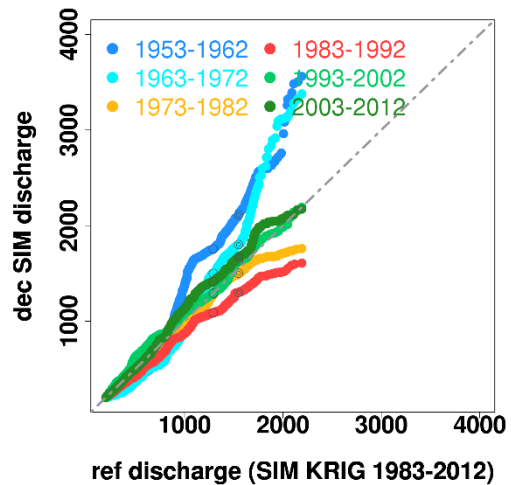
2 Figure 10: Quantile-Quantile plot of the Red flood period distribution of daily discharge of
3 each decade between 1953 and 2012. The x axis is for observations and the y axis for the
4 simulations.

5

a- QQplot observed Niamey discharge



b- QQplot discharge Niamey KRIG

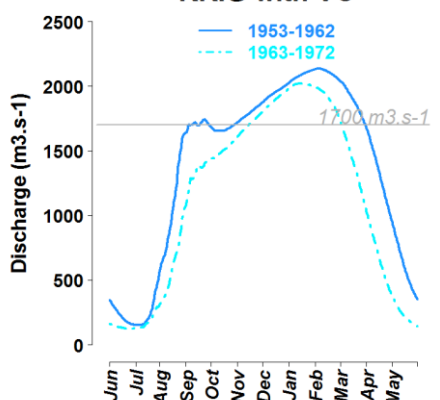
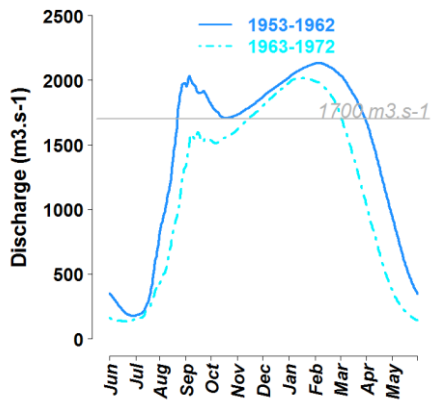


1

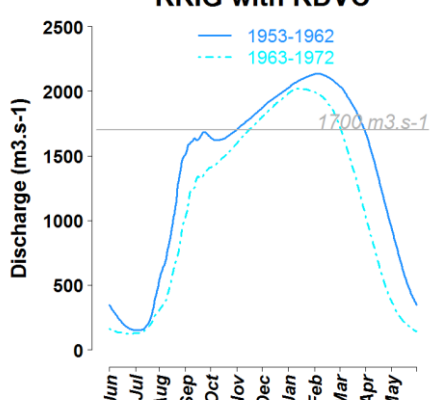
2 Figure 11: Quantile-Quantile plot of the distribution of daily discharge in Niamey (observed
3 in a; simulated in b) for each decade since 1953; the reference (x axis) is the Red flood
4 observed/simulated daily discharge between 1983 and 2012.

5

1 a- Niamey simulated discharge
KRIG with RC

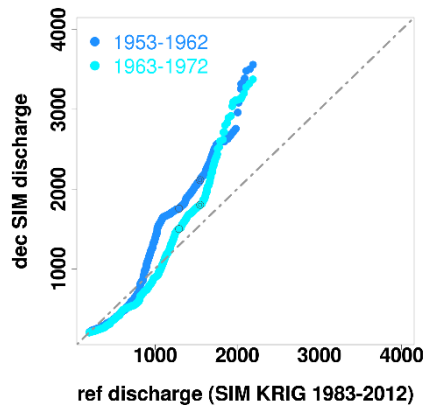


3 c- Niamey simulated discharge
KRIG with RDVC

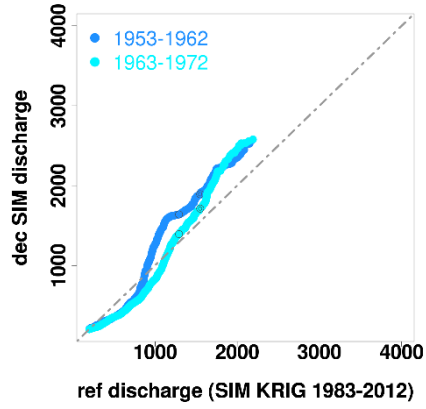


4 Figure 12: simulated decadal mean discharge in Niamey with 3 scenarii: (a) recent surface
5 condition (RC), (b) fully vegetated basin condition (VC) and (c) fully vegetated basin with
6 smaller drainage area condition (VCRD).

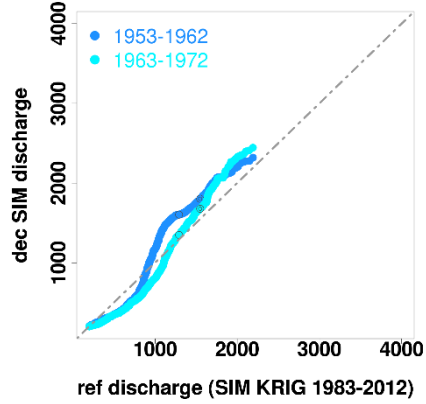
1 a- QQplot discharge Niamey KRIG



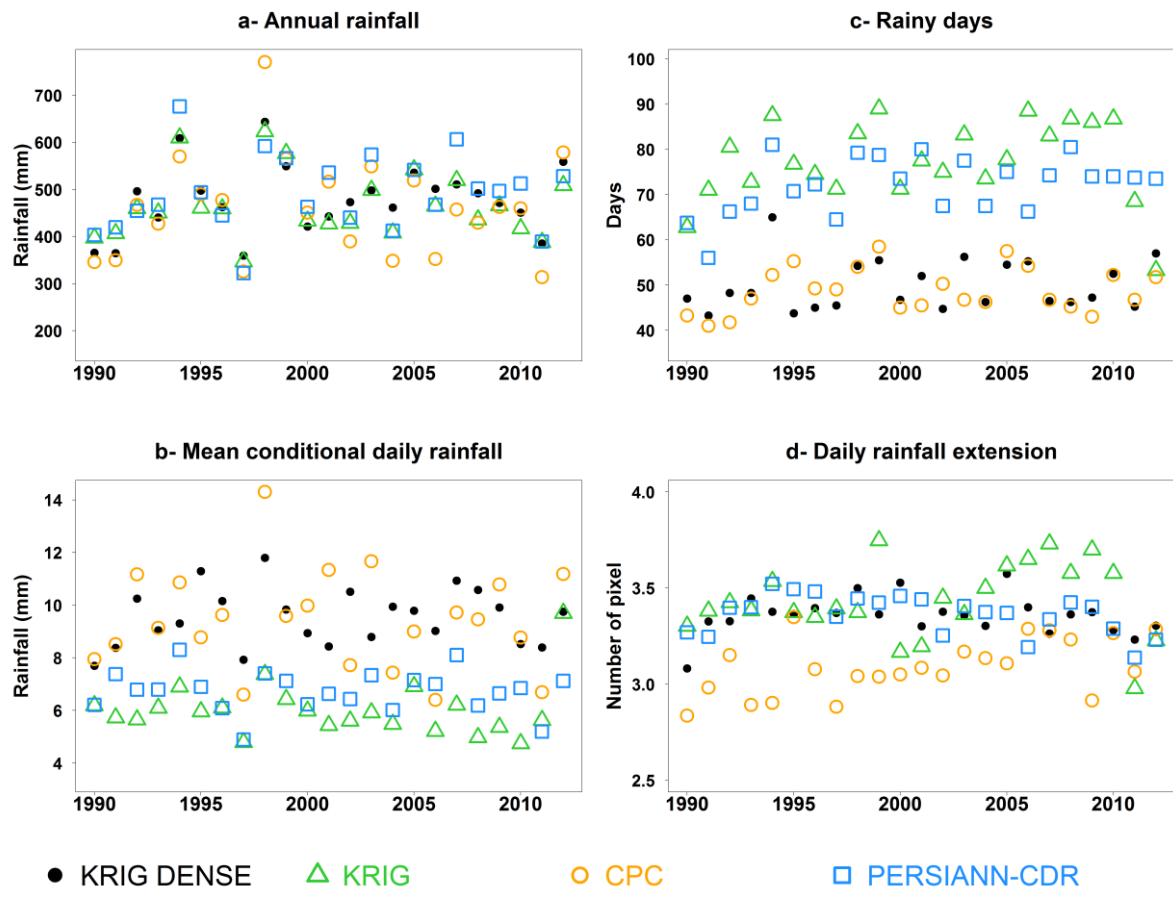
2 b- QQplot discharge Niamey KRIG
vegetalised area



3 c- QQplot discharge Niamey KRIG
vegetalised and small area



4 Figure 13: Quantile-Quantile plot of daily annual discharge of each decade, the reference is
5 daily discharge between 1983 and 2012.



1 ● KRIG DENSE ▲ KRIG ○ CPC □ PERSIANN-CDR
2 Figure A1: Annual (JJAS) series of rainfall characteristics between 1990-2012 compute for
3 the reference (KRIG-DENSE, black dots) and the 3 tested products : KRIG open (green
4 triangle), CPC (open orange circle) and PERSIANN-CDR (open blue square). a) presents the
5 mean annual rainfall amount series, b) presents the annual number of rainy day, c) presents
6 the mean conditional daily rainfall series and d) presents the mean of rain extension over the
7 studied area (in pixel).